

# Exploring the Effects of Lignin Nanoparticles in Different Zebrafish Inflammatory Models

Cinzia Bragato<sup>1</sup>, Andrea Persico<sup>1</sup>, Guillem Ferreres<sup>2</sup>, Tzanko Tzanov<sup>2</sup>, Paride Mantecca<sup>1</sup>

<sup>1</sup>POLARIS Research Center, Department of Earth and Environmental Sciences, University of Milano-Bicocca, Milan, 20126, Italy; <sup>2</sup>Group of Molecular and Industrial Biotechnology, Universitat Politècnica de Catalunya, Terrassa, 08222, Spain

Correspondence: Cinzia Bragato, Piazza della Scienza 1, Milan, 20126, Italy, Tel +39 0264482928,, Email [cinzia.bragato@unimib.it](mailto:cinzia.bragato@unimib.it)

**Purpose:** Lignin is the most abundant source of aromatic biopolymers and has gained interest in industrial and biomedical applications due to the reported biocompatibility and defense provided against bacterial and fungal pathogens, besides antioxidant and UV-blocking properties. Especially in the form of nanoparticles (NPs), lignin may display also antioxidant and anti-inflammatory activities.

**Methods:** To evaluate these characteristics, sonochemically nano-formulated pristine lignin (LigNPs) and enzymatically-phenolated one (PheLigNPs) were used to expose zebrafish embryos, without chorion, at different concentrations. Furthermore, two different zebrafish inflammation models were generated, by injecting *Pseudomonas aeruginosa* lipopolysaccharide (LPS) and by provoking a wound injury in the embryo caudal fin. The inflammatory process was investigated in both models by qPCR, analyzing the level of genes as *il8*, *il6*, *il1β*, *tnfa*, *nfkbiaa*, *nfk2*, and *ccl34a.4*, and by the evaluation of neutrophils recruitment, taking advantage of the Sudan Black staining, in the presence or not of LigNPs and PheLigNPs. Finally, the *Wnt/β-catenin* pathway, related to tissue regeneration, was investigated at the molecular level in embryos wounded and exposed to NPs.

**Results:** The data obtained demonstrated that the lignin-based NPs showed the capacity to induce a positive response during an inflammatory event, increasing the recruitment of cytokines to accelerate their chemotactic function. Moreover, the LigNPs and PheLigNPs have a role in the resolution of wounds, favoring the regeneration process.

**Conclusion:** In this paper, we used zebrafish embryos within 5 days post fertilization (hpf). Despite being an early-stage exemplary, the zebrafish embryos have proven their potential as predicting models. Further long-term experiments in adults will be needed to explore completely the biomedical capabilities of lignin NPs. The results underlined the safety of both NPs tested paved the way for further evaluations to exploit the anti-inflammatory and pro-healing properties of the lignin nanoparticles examined.

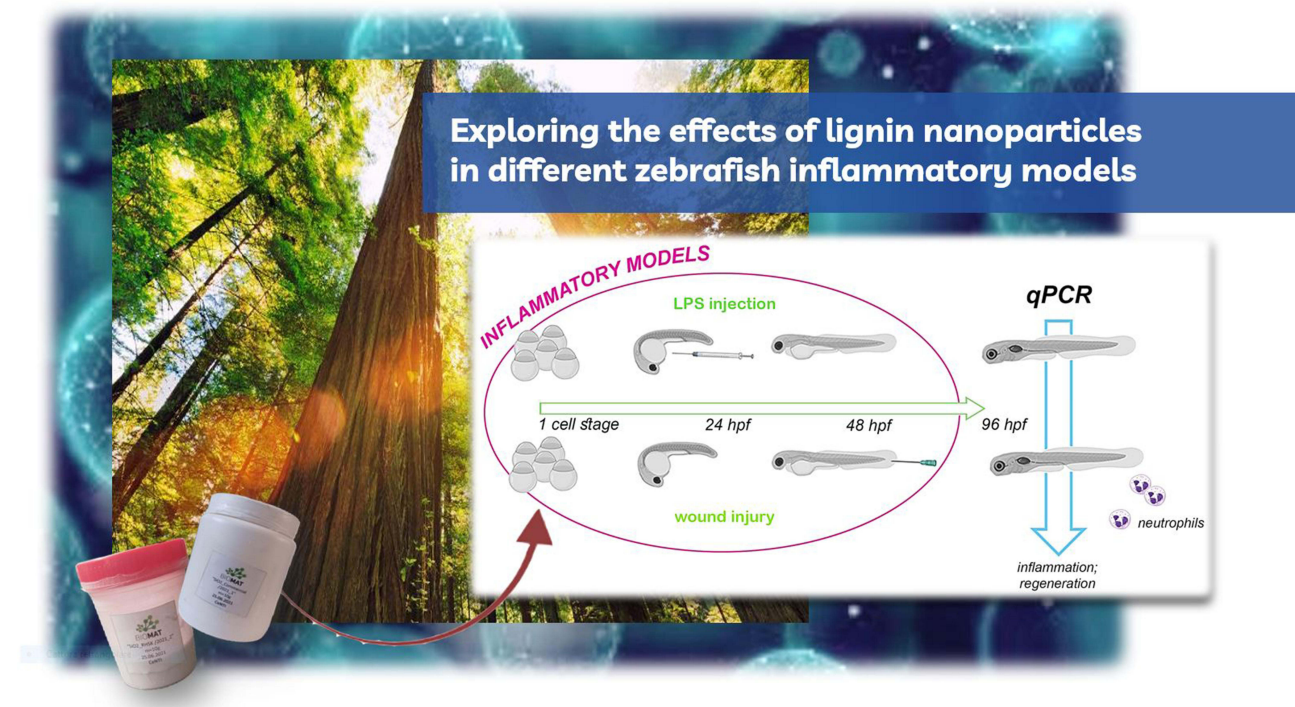
**Keywords:** bio-based nanoparticles, zebrafish embryo, inflammation, LPS, wound

## Introduction

Lignin is the most abundant sustainable source of aromatic biopolymers, representing 15–30% of the plants' dry mass. Every year, the paper manufacturing industry generates nearly 70 million tons of lignin as a low-value by-product usually used for energy recovery or discarded as a waste liquid.<sup>1</sup> Only 2–5% of lignin is revalorized in its macromolecular form and commercialized as an additive in adhesive formulations and polyurethanes or as a surfactant for colloidal suspensions.<sup>2</sup>

Recently, lignin has gained interest even in industrial and biomedical applications. In fact, due to the presence of phenolic hydroxyl groups in its structure, it provides defense against bacterial and fungal pathogens,<sup>3</sup> besides antioxidant<sup>4</sup> and UV-blocking properties.<sup>5</sup> Furthermore, these phenolic functionalities allow further modification of lignin, enabling different applications as an active ingredient, especially in the form of nanoparticles (NPs).<sup>6</sup> Lignin nanoparticles (LigNPs) have been lately used in polymeric materials as mechanical reinforcement, UV absorbents, antibacterial and antioxidant agents in food packaging, and carriers for drug delivery. Extensive attempts have been made to propose possible uses of lignin waste as fillers for the preparation of polyurethane foams, fiber mats, and thermoplastics materials, due to its multiple characteristics, such as the high abundance, low weight, carbon neutrality,

## Graphical Abstract



biodegradability, and reinforcing capability.<sup>6</sup> Even if all these features seem to make lignin the perfect material, given the fact that it is natural, present almost everywhere, and plentiful, there are reasons explaining its limited use and applicability. For instance, lignin presents low compatibility with polymeric matrices in composite production and a heterogeneous molecular structure.

In this frame, the effort of researchers led to the understanding that some factors, such as the sonication time and amplitude, lignin concentration, and flow rate, can improve the industrial process for lignin nano-transformation.<sup>6</sup> In addition, taking advantage of a sono-enzymatic approach for the simultaneous functionalization and nano-transformation of lignin, recently, phenolated lignin nanoparticles (PheLigNPs) with antimicrobial efficacy have been produced, without the need for chemical modification or combination with metals, usually required to potentiate the antimicrobial properties of lignin.<sup>7</sup>

Phenolation and amination are techniques used to enhance the antibacterial and antioxidant properties of LigNPs. However, these strategies often involve toxic reagents or metal catalysts and require harsh conditions<sup>7-10</sup> proposed an eco-friendly enzymatic approach for grafting functional molecules onto lignin, thereby improving its performance in specific applications, eg as an antimicrobial agent or as a reinforcing element in composite materials. This biotechnological approach provides clear advantages over chemical modifications, in particular at the environmental level, avoiding the use of hazardous reagents and reducing toxic wastes.<sup>7</sup>

Besides the known antioxidant activity of lignin, different biological capabilities characterize this material. For instance, the great number of S and G phenylpropane groups, ample phenolic hydroxyl groups, and lower molecular weight are features that give lignin the ability to scavenge free radicals and reactive oxygen species (ROS).<sup>11</sup> In addition to antioxidant, antibacterial, and anti-UV properties, it is reported that lignin possesses anti-inflammatory<sup>12</sup> and neuroprotective properties.<sup>13</sup> In this context, the evaluation of new and different properties, such as the possible anti-inflammatory abilities of completely natural PheLigNPs appears very attractive for biomedical purposes.

Many papers can be found in the most recent literature describing the attempt to use lignin as a bio-material in the medical field, since products from plants typically present excellent biocompatibility. However, despite of the growing research on biomedical applications of lignin-based materials, and in particular LigNPs, such materials still lack regulatory approval and standardization partially due to intrinsic heterogeneity and additional structural changes during their extraction.<sup>14–19</sup> There are research works on the use of lignin nanoparticles as drug delivery in cancer,<sup>20</sup> or as treatment for different pathologies,<sup>21</sup> but most of the data are obtained in in vitro models. Despite the uncontested utility of the in vitro systems, there is a lack of in vivo evaluations in reliable and accessible animal models.

In this contest, the use of zebrafish (*Danio rerio*) model can be useful to observe an integrated biological response that takes into consideration different aspects.<sup>22</sup> For these reasons, the zebrafish embryos were used to test in vivo the effects of LigNPs and PheLigNPs in two distinct inflammatory situations - one induced by a lipopolysaccharide (LPS) injection, and the other caused by wounding. Zebrafish, a Teleostei fish member of the *Cyprinidae* family, has been widely used as a research organism since the 1960s. It possesses a unique combination of features, such as high fecundity, optical transparency, extra-uterine fecundation, rapid development, and easy genetic manipulation, that make this little fish amenable to many research fields. Moreover, it can be considered as a credible translational and predictive model.<sup>23,24</sup> Zebrafish has been employed so far as a model organism for in vivo illness modeling and evaluation of medicine and plant-derived extractives since the hematopoietic system and the immune cell types are similar to the human ones.<sup>25</sup> Furthermore, zebrafish has been largely implied as an inflammation model, since it is highly influenced by different types of external injuries, and consequently more susceptible to inflammation.<sup>26</sup>

Furthermore, zebrafish embryos are a powerful system for assessing skin inflammatory responses at the early life stages.<sup>27</sup>

In this work, different techniques were used to evaluate the anti-inflammatory effects of PheLigNPs, compared to unmodified LigNPs, on zebrafish embryos. At first, the NPs were characterized by transmission electron microscopy (TEM) and dynamic light scattering (DLS). Successively, after the screening of lethal and malformation effects through the ISO/TS 22082:2020 (Nanotechnologies — Assessment of nanomaterial toxicity using dechorionated zebrafish embryo) (<https://www.iso.org/standard/72516.html>), a panel of genes, such as *tnfa*, *nfbk2*, *il8*, *il6*, *il1β*, *nfbkaa*, and *ccl34a.4*, were evaluated by qRT-PCR after both inflammatory models' generation (LPS injection or wound) (Figure 1).

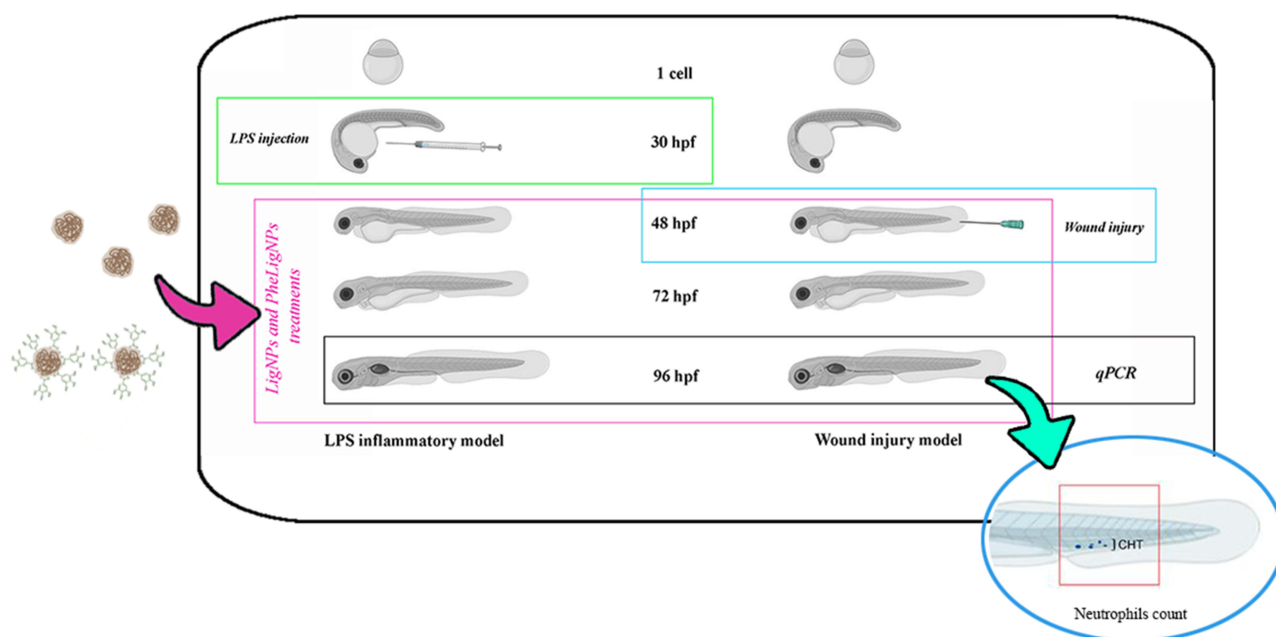


**Figure 1** Experimental plan. Two lignin nanoparticles sono-enzymatically extracted were used, i) non-functionalized (LigNPs), and ii) functionalized with phenols groups derived from tannic acid (PheLigNPs). Both nanoparticles were produced with the intent of being used as additives for adhesives, in polyurethane foams, as surfactants in colloidal suspensions and for food packaging. Since it is reported that several polyphenolic compounds derived from plant extracts have anti-inflammatory properties we decided to investigate whether LigNPs and PheLigNPs could have effects on modulating the inflammatory response in two different inflammatory models (embryos LPS-injected or wounded) Both models were compared at molecular level, undergoing to the same time-exposure to LigNPs and PheLigNPs.

Sudan Black b histochemical staining was used to evaluate the recruitment of neutrophils after wound and successive exposure to NPs. Finally, the capability of LigNPs and PheLigNPs to modulate the Wnt/ $\beta$ -catenin signaling pathway was studied, to explore the possibility that these NPs could promote tissue re-generation. In this research, new beneficial properties of lignin and phenolated lignin nanoparticles were reported in vivo for the first time, underlining the incredible potential and applicability that this natural material can have in a variety of areas, and in particular the biomedical field.

## Materials and Methods

### Synthesis and Morphological and Surface Characterization of LigNPs and PheLigNPs

Protobind™ 6000 soda lignin was purchased from PLT Innovations (Switzerland). Tannic acid (TA), gallic acid (GA), and 3',5'-dimethoxy-4'-hydroxyacetophenone (acetosyringone) were supplied by ACROS Organics (Belgium). Fungal laccase Novozym 51003 from *Myceliophthora thermophila* (EC1.10.3.2) was obtained from Novozymes (Denmark). Folin-Ciocalteu phenol reagent was purchased from Sigma-Aldrich (Spain).

Pristine lignin, Protobind™ 6000 soda lignin (PLT Innovations, Switzerland) was enzymatically modified using a laccase-mediator-assisted approach. First, a 1.5 g/L acetosyringone (ACROS organic, Belgium) solution in pH 5.5 50 mM acetate buffer was prepared, and 30 g/L of lignin was added to the mixture. After complete homogenization, 6 U/mL of fungal laccase Novozym 51003 from *Myceliophthora thermophila* (EC1.10.3.2) (Novozymes, Denmark) was added to the solution. The biomass was pre-activated for 1 h before the functionalization. Subsequently, the phenolic compounds tannic acid (TA) and gallic acid (GA) (ACROS organic, Belgium) were incorporated into the reaction at a concentration of 18 g/L for each reagent. The functionalization reaction was carried out for 2 h at 300 rpm of agitation and 40 °C. Finally, the unreacted precursors were separated by centrifugation at 15000 g for 20 min and the phenolated lignin in the pellet was freeze-dried for 2 days. The successful modification of lignin was assessed by Fourier-transform infrared spectroscopy (FTIR). Prior to the analysis, the NPs were lyophilized at – 80°C and 0.2 bars for 36 hours in a freeze-dryer LyoAlfa 15 (Telstar, Spain) to remove the water from the samples. FTIR was conducted with a PerkinElmer Spectrum 100 instrument (PerkinElmer, USA). Spectra were acquired over a wavenumber range of 4000–650  $\text{cm}^{-1}$ , performing 64 scans. Baseline correction and normalization were carried out with PerkinElmer Spectrum software. The phenolic content increase was assessed using the Folin-Ciocalteu phenol reagent (Sigma-Aldrich, Spain). 20  $\mu\text{L}$  of lignin solution at a concentration of 1 mg/mL was mixed with 100  $\mu\text{L}$  of 20%  $\text{Na}_2\text{CO}_3$  and 80  $\mu\text{L}$  of 0.2 N Folin-Ciocalteu reagent. After 10 min of incubation, the absorbance changes at 765 nm were measured and the phenolic content was calculated using a TA calibration curve.

The nano-transformation of pristine and modified lignin was carried out as previously described.<sup>6</sup> Briefly, 30 g/L biomass dispersion was recirculated at a flow rate of 222 mL/min through a 500 mL cylindrical sonochemical flow cell (Sonics & Materials, Inc., USA) operating at 50% amplitude and equipped with a jacket to maintain the reaction temperature at 50 °C for 2 h. The LigNPs and PheLigNPs were recovered by centrifugation at 18000 g for 30 min and freeze-dried for 2 days.

Transmission electron microscopy (TEM) was used to study the morphology of the NPs by placing 10  $\mu\text{L}$  of water-diluted samples on a carbon-coated 300-mesh copper grid. Grids were observed with a Jeol JEM 2100Plus (JEOL, Tokyo, Japan) TEM, operating at an acceleration voltage of 200 kV and equipped with an 8 MPx complementary metal oxide semiconductor (CMOS) Ga-tan Rio9 (Gatan, Pleasanton, CA, USA) digital camera.

The hydrodynamic size distribution of LigNPs and PheLigNPs was evaluated through dynamic light scattering (DLS) analysis using a Malvern Zetasizer S90 (Malvern Instruments Inc., U. K). The NP hydrodynamic behavior was assessed after dispersing the NPs (final concentration 100 mg/L) in two different media: i) Milli-Q (mQ) water and ii) FET solution (0.1 g  $\text{NaHCO}_3$  and 0.19 g  $\text{CaSO}_4 \cdot 2\text{H}_2\text{O}$ ; from Sigma-Aldrich, St. Louis, Missouri, MO, USA; 0.1 g instant ocean from Instant Ocean Spectrum Brands, Blacksburg, Virginia, VA, USA).

## Animal Care

The adults AB wildtype are maintained and bred at the University of Milan-Bicocca zebrafish facility (approved by ATS Metro Milano Prot. n. 0020984—12 February 2018), in a recirculating ZebTec Active Blue aquatic system (Tecniplast,



Buguggiate, Italy). All experiments were performed on embryos within 5 days post fertilization (dpf), thus not subject to animal experimentation rules according to European and Italian directives. Embryos were raised at 28°C and staged according to Kimmel et al.<sup>28</sup>

## Streptomyces Griseus Pronase Treatment

The pronase (EC 3.4.24.4; CAS# 9036–06-0, Sigma Aldrich) is an enzyme mixture of several non-specific endo and exo proteases that digest proteins down to single amino acids, from *Streptomyces griseus*. Briefly, the pronase was resuspended and divided into small volumes. The working solution used was 10 mg/mL concentrated. The 6 hpf developmental stage selected embryos were incubated with pronase in a Petri glass dish for 30 seconds at room temperature (RT), applying gentle shaking under a stereomicroscope. After that embryos were rapidly and frequently washed with FET solution (0,1 g of NaHCO<sub>3</sub>; 0.1 g of Instant Ocean; 0.19 g of CaSO<sub>4</sub>\*2 H<sub>2</sub>O for 1L of solution) at least 6 or 7 times. If some chorions were still intact, a mechanical rupture of it, by the use of needles, was provided. Finally, the embryos were recovered and exposed to LigNPs and PheLigNPs at different concentrations.

## Embryonic Zebrafish Assay. ISO/TS 22082:2020 Nanotechnologies — Assessment of Nanomaterial Toxicity Using the Dechorionated Zebrafish Embryo

Since the chorion plays a role in protecting the embryo from external influences, we removed the chorion to facilitate a toxicological assessment that is more indicative of direct exposure to the NPs studied. The evaluation was conducted according to the International Organization for Standardization (ISO) TS 22082:2020 guidelines. Briefly, freshly fertilized zebrafish embryos were exposed to contaminants for a total of 96 h, after dechoriation treatment with pronase enzyme.

The NPs in solution form were diluted in FET medium to the desired concentration (0.1, 1, 10, 50, and 100 mg/L). Every 24 h, embryos were screened for lethality, in particular checking coagulation of fertilized eggs, lack of somite formation, lack of detachment of the tail bud from the yolk sac, and lack of heartbeat, according to the specific time points. Moreover, sub-lethal endpoints, such as reduced yolk resorption, blood congestion, and formation of edema were observed from 48 hours post-fertilization (hpf) to 96 hpf developmental stage. At the end of the exposure period, the embryos were divided into groups, to be processed for morphometric, molecular, and histochemical analyses. The embryos were observed during 5 different experiments, in which n = 24 embryos were exposed for each condition (0.1, 1, 10, 50, and 100 mg/L) and compared to n = 24 control embryos not exposed. The total number of embryos observed at the end of the 5 experiments was n = 120 embryos for each condition, compared to n = 120 control embryos not exposed.

## LPS-Induced Inflammatory Model

The microinjection of *P. aeruginosa* lipopolysaccharide (LPS) (derived from strain ATCC 27316, Sigma Aldrich) was used to generate a model of acute inflammation in zebrafish embryos.<sup>10</sup> Embryos at 30 hpf were microinjected with 1 nL of 250 µg/mL of LPS suspension into the apical portion of the yolk sac. Embryos were incubated at 28.5°C in FET solution to which was added 0.003% 1-phenyl-2-thiourea (PTU, Sigma-Aldrich, Saint Louis, MO) to prevent pigmentation. The experimental groups observed were i) embryos not injected (negative Ctrl); ii) embryos LPS-injected (LPS, positive control); iii) embryos LPS-injected and exposed to LigNPs (100 mg/L); iv) embryos LPS-injected and exposed to PheLigNPs (100 mg/L); v) embryos not injected and exposed to LigNPs (100 mg/L) (Ctrl LigNPs); and vi) embryos not injected and exposed to PheLigNPs (100 mg/L) (Ctrl PheLigNPs) for 48 hours. At 96 hpf, n = 45 embryos per condition, pertaining to 3 different experiments, were used for molecular analyses, including the evaluation of *tnfa*, *nfkβ2*, *il8*, *il6*, *il1β*, *nfkbiaa*, *ccl34a.4* expression levels.

## Wound-Induced Inflammatory Model

Anesthetized wild-type larvae were wounded at 48 hpf by a microneedle, causing a cut directly in the caudal fin. Wounded larvae were then randomly divided into 4 experimental groups, such as i) Ctrl not wounded; ii) Ctrl wounded; iii) Embryos wounded and exposed to LigNPs (100 mg/L), and iv) Embryos wounded and exposed to PheLigNPs (100 mg/L). The embryos after wounding, exposed or not to lignin NPs, were placed at 27 ± 1°C. Every 24 hours, embryos were placed in a 60 mm Petri dish with a medium containing 0.016% ethyl 3-aminobenzoate methanesulfonate

salt (Tricaine, Sigma-Aldrich), and a single-plane image was acquired using Leica M205FA microscope equipped with a 5MPx DFC450C digital camera and Leica software (Leica). Larvae were rinsed, placed into fresh FET solution, with or without NPs, and returned to  $27 \pm 1^\circ\text{C}$  until subsequent imaging. The tissue regrowth area was photographed over time. At the end of the experiment,  $n = 30$  embryos per condition, pertaining to 3 different experiments, were used for the molecular analyses, including the evaluation of *tnfa*, *nfk2*, *il8*, *il6*, *il1 $\beta$* , *nfkbiaa*, *ccl34a.4*, *wnt4a*, *gsk3 $\beta$* , *wnt10b*, and  *$\beta$ -catenin* expression levels, while 15 embryos per experiment were used for the evaluation of neutrophils number.

## RNA Extraction

Total RNA was isolated from zebrafish embryos ( $n = 15$  embryos randomly collected, for each exposure condition and in each experiment) using TRIzol reagent (15596018, Invitrogen). First-strand cDNA synthesis reaction from total RNA was catalyzed by LunaScript<sup>®</sup> RT SuperMix Kit (New England Biolabs, Ipswich, MA, USA). cDNA was amplified with specific primers using Phusion High-Fidelity polymerase (Finnzymes, Thermo Fisher Scientific, Waltham, MA, USA).

## qRT-PCR: Analyses of Relative Gene Expression Level

Quantitative real-time PCR (qRT-PCR) was performed using Luna<sup>®</sup> Universal qPCR Master Mix kit (New England Biolabs, Ipswich, MA, USA), using the Quantum 3<sup>™</sup> (Applied Biosystems, Waltham, MA, USA) Real-Time PCR system, according to manufacturer instructions. Briefly, real-time PCR was performed in a 10  $\mu\text{L}$  reaction containing 600 nM of each primer, 2  $\mu\text{L}$  template cDNA, and 5  $\mu\text{L}$  qPCR Master Mix. The PCR was run at  $95^\circ\text{C}$  for 60 sec followed by 40 cycles of  $95^\circ\text{C}$  for 15 sec and  $60^\circ\text{C}$  for 30 sec. *lsm12b* or *mobk13* were used as the endogenous control. Relative changes in gene expression between control and treated samples were determined using the  $2^{-\Delta\Delta\text{Ct}}$  method, and the results were presented in a logarithmic scale (log 2-fold change). The primer sequences of tested genes (*tnfa*, *nfk2*, *il8*, *il6*, *il1 $\beta$* , *nfkbiaa*, *ccl34a.4*, *wnt4a*, *gsk3 $\beta$* , *wnt10b* and  *$\beta$ -catenin*) are listed in [Additional Table 1](#).

## Sudan Black B Staining

To mark the mature neutrophils, we used the Sudan Black histochemical staining, as previously described.<sup>29</sup> We prepared the buffer solution with crystalline phenol (16 g), absolute ethanol (30 mL), and double distilled water (100 mL) plus  $\text{Na}_2\text{HPO}_4 \cdot 12\text{H}_2\text{O}$  (0.3 g). The Sudan black stock solution was prepared by dissolving 0.3 g of Sudan black powder (0.3 g) into absolute ethanol (100 mL), under stirring for 48 hours at RT. The working staining solution (SB) was made by mixing stock solution (30 mL) with buffer (20 mL) and filtering. The embryos ( $n = 15$  embryos, randomly collected for each exposure condition and in each experiment) were fixed with 4% methanol-free paraformaldehyde (PFA) in PBS for 2 hours at room temperature, rinsed in PBS several times, incubated in SB for 20 minutes at RT, washed extensively in 70% ethanol in water, then progressively rehydrated with PBS plus 0.1% Tween-f20 (PBST).

## Neutrophils Quantification

To quantify the Sudan black staining, embryos were observed under a stereo microscope, and pictures of the entire tail, starting from the caudal hematopoietic tissue (CHT) area, were collected. The purple signal area (expressed as arbitrary units) was calculated by ImageJ Fiji software (<https://imagej.net/Fiji>) on Bright-field images taken under the same conditions, such as light exposition and frame size. Using the software, a threshold was applied to the pictures to obtain regions positive for Sudan black in black and negative in white. Automatic particle counting was then applied in the pictures, launching the “Cell Counter” plugin, developed by Wayne Rasband.<sup>30,31</sup>

## Statistical Analysis

Data are reported as means and standard error of the means (SEM) using GraphPad Prism 9.2.0.332 (GraphPad Software). To determine the statistical significance between multiple groups, we employed one-way ANOVA, followed by Bonferroni's post hoc test analysis. We considered the level of significance at  $p < 0.05$ .

The data presented were obtained from embryos collected during each experiment from at least 3 mating tanks, containing 5 females and 5 males per tank. Each replicate was conducted separately, during different days or weeks.

## Results

### Physic-Chemical Evaluation of LigNPs and PheLigNPs

To assess the modification of lignin, lignin, and phenolated lignin were analyzed by FTIR. The presence of TA and GA in the spectrum of the modified lignin was demonstrated by the increase of the  $-OH$  signal at the region between  $3000-3600\text{ cm}^{-1}$ , associated with the stretching vibration of hydroxyl groups, an increase in the signal at  $1340\text{ cm}^{-1}$ , corresponding to phenolic groups, and the increase of  $-CH$  groups detected at  $2850$  and  $2930$ , and  $760\text{ cm}^{-1}$ .<sup>32</sup> The grafting of the phenolic compounds on the biomass was confirmed by the strong peak at  $1720\text{ cm}^{-1}$ , corresponding to the stretching vibration of  $C=O$  bonds (Figure 2A).<sup>7,30,33</sup> Additionally, the phenolic content of the phenolated lignin increased by more than 50%, from  $0.88\text{ }\mu\text{mols}$  of TA per mg of biomass to  $1.36\text{ }\mu\text{mols}$  of TA per mg.

The LigNPs and PheLigNPs were investigated morphologically by transmission electron microscopy (TEM images). The electron micrographs obtained showed agglomeration of nanoparticles in both lignin and phenolated lignin (Figure 2).

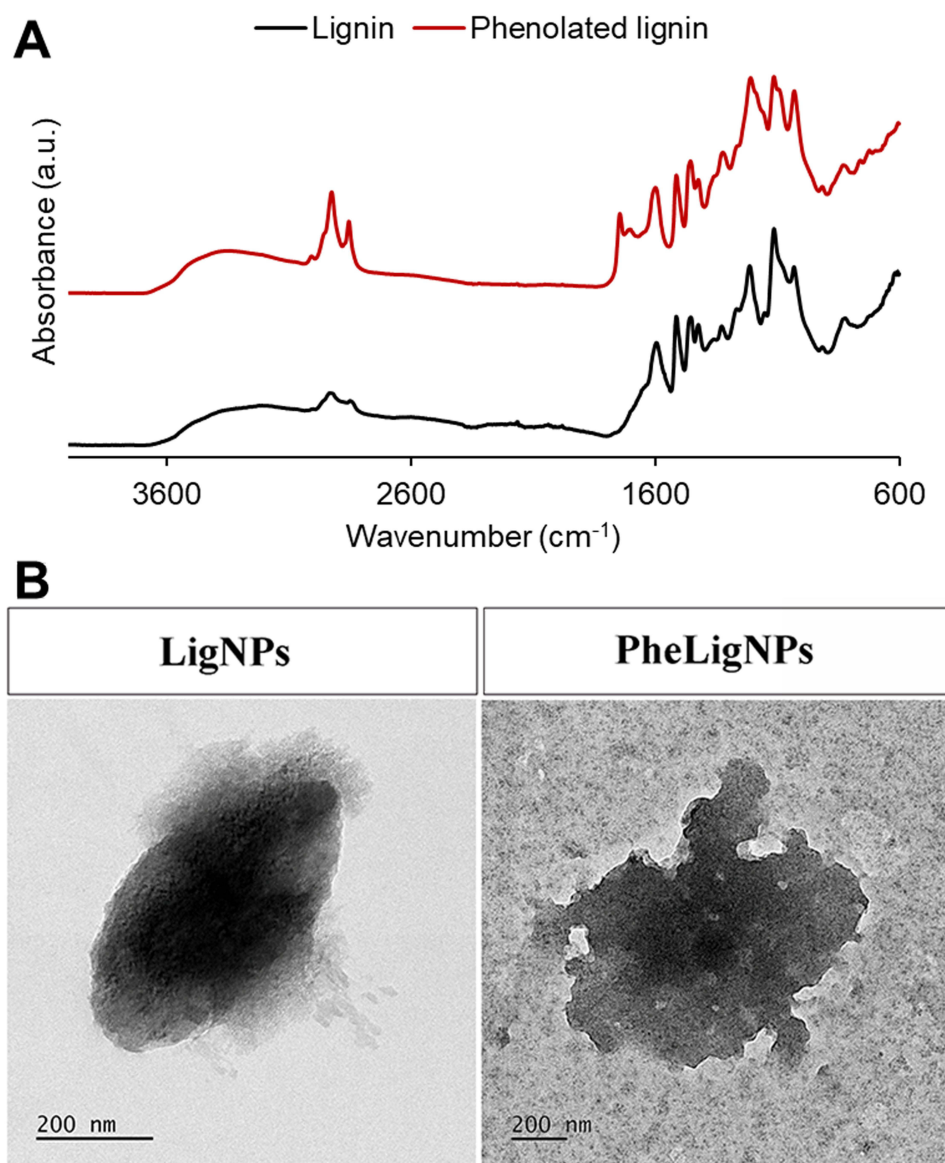


**Figure 2 (A)** FTIR analysis of the pristine and phenolated lignin. **(B)** Electron micrographs of LigNPs and PheLigNPs.

**Table 1**  $\zeta$ -Average (nm) and Polydispersity Index (Pdl) of 100 Mg/L LigNPs and PheLigNPs Measured by Dynamic Light Scattering (DLS) at Different Time Point and in Different Media (mQ Water and FET Solution). Means SD of Three Replicates

NPs (100 mg/L)	Medium	Time (h)	$\zeta$ -Average (nm) $\pm$ SD	Pdl $\pm$ SD	$\zeta$ -Pot (mV) $\pm$ SD
LigNPs	mQ	0	355.5 $\pm$ 7.366	0.197 $\pm$ 0.017	-33.2 $\pm$ 2.5
	mQ	24	293.0 $\pm$ 4.456	0.172 $\pm$ 0.043	
	mQ	48	300.8 $\pm$ 6.657	0.122 $\pm$ 0.06	
	mQ	72	301.2 $\pm$ 3.900	0.134 $\pm$ 0.027	-31 $\pm$ 0.1
	FET	0	384.0 $\pm$ 7.725	0.196 $\pm$ 0.055	-19.7 $\pm$ 0.416
	FET	24	314.7 $\pm$ 8.554	0.116 $\pm$ 0.017	
	FET	48	286.3 $\pm$ 0.650	0.149 $\pm$ 0.022	
	FET	72	292.1 $\pm$ 7.427	0.122 $\pm$ 0.034	-17.1 $\pm$ 0.451
PheLigNPs	mQ	0	525.4 $\pm$ 23.290	0.345 $\pm$ 0.016	-32.7 $\pm$ 0.451
	mQ	24	568.9 $\pm$ 10.060	0.099 $\pm$ 0.015	
	mQ	48	526.0 $\pm$ 15.970	0.221 $\pm$ 0.009	
	mQ	72	500.0 $\pm$ 3.301	0.181 $\pm$ 0.023	-30.7 $\pm$ 0.781
	FET	0	564.1 $\pm$ 7.911	0.334 $\pm$ 0.073	-16.5 $\pm$ 0.902
	FET	24	503.7 $\pm$ 20.020	0.21 $\pm$ 0.037	
	FET	48	482.5 $\pm$ 8.429	0.168 $\pm$ 0.024	
	FET	72	452.3 $\pm$ 8.951	0.197 $\pm$ 0.017	-16.3 $\pm$ 0.551

Data from DLS analyses, performed in two different media (mQ water and FET medium) and at different time points (0, 24, 48, and 72 hours), showed that LigNPs and PheLigNPs were relatively stable when resuspended in both solutions. The hydrodynamic size of LigNPs resuspended in mQ water was 355.5  $\pm$  7.366 nm at 0 h, while the hydrodynamic size at 72 h was 301.2  $\pm$  3.900 nm, while the size presenting after resuspension in FET solution was 384.0  $\pm$  7.725 at time 0 hours (h), and 292.1  $\pm$  7.427 nm at 72 h. Regarding PheLigNPs, the size in mQ water was 525.4  $\pm$  23.290 nm at 0 hours and 500  $\pm$  3.301 nm at 72 h, while in FET solution was 564.1  $\pm$  7.911 nm and 452.3  $\pm$  8.951 nm at 0 and 72 h, respectively (Table 1). The polydispersion index (Pdl) measurement of both LigNPs and PheLigNPs at 0 and 72 h showed similar values (for LigNPs, an average of 0.156  $\pm$  0.036 in mQ, and 0.145  $\pm$  0.032 in FET medium; while for PheLigNPs, an average of 0.211  $\pm$  0.015 in mQ and 0.227  $\pm$  0.037 in FET medium), highlighting the fact that the NPs were mono-dispersed. The  $\zeta$ -potentials, measured in mQ water of LigNP (equal to -33.20 mV at 0 h and -31 mV at 72 h) and of PheLigNP (equal to -32.40 mV at 0 and -30.7 mV at 72 h), showed that these NPs were negatively charged and colloiddally stable. The  $\zeta$ -potential measured in the FET solution, even though still negative, presented a reduced charge for both NPs. For instance, LigNPs showed a  $\zeta$ -potential of -19.7 mV at 0 h and -17.1 mV at 72 h, while PheLigNPs had -16.5 mV at 0 h and -16.3 mV at 72 hours.

## Assessment of the Effects of LigNPs and PheLigNPs on Dechorionated Zebrafish Embryo

The effects after exposure to LigNPs and PheLigNPs were assessed during three static tests, starting from the 80% epiboly developmental stage, after chemical chorion deprivation (Figure 3). The pronase treatment, used for this purpose, caused a mortality rate of around 27%, a percentage attributable probably to the treatment itself<sup>34</sup> (Figure 3A).

After exposure of 96 h, the embryos were fixed in 4% paraformaldehyde (PFA) and measured to observe statistically significant morphological defects. The body length, the eye area, the eye diameter, the yolk area, and the eye distance were calculated. The results showed no significant lethal and malformation effects on embryos exposed to both NPs at different concentrations, compared to control embryos (Ctrl) (Figure 3B–3F). The few malformations detected were pertinent to body axis defects, in a percentage of less than 4%, observed at the end of the experimental exposure time (96 hpf).



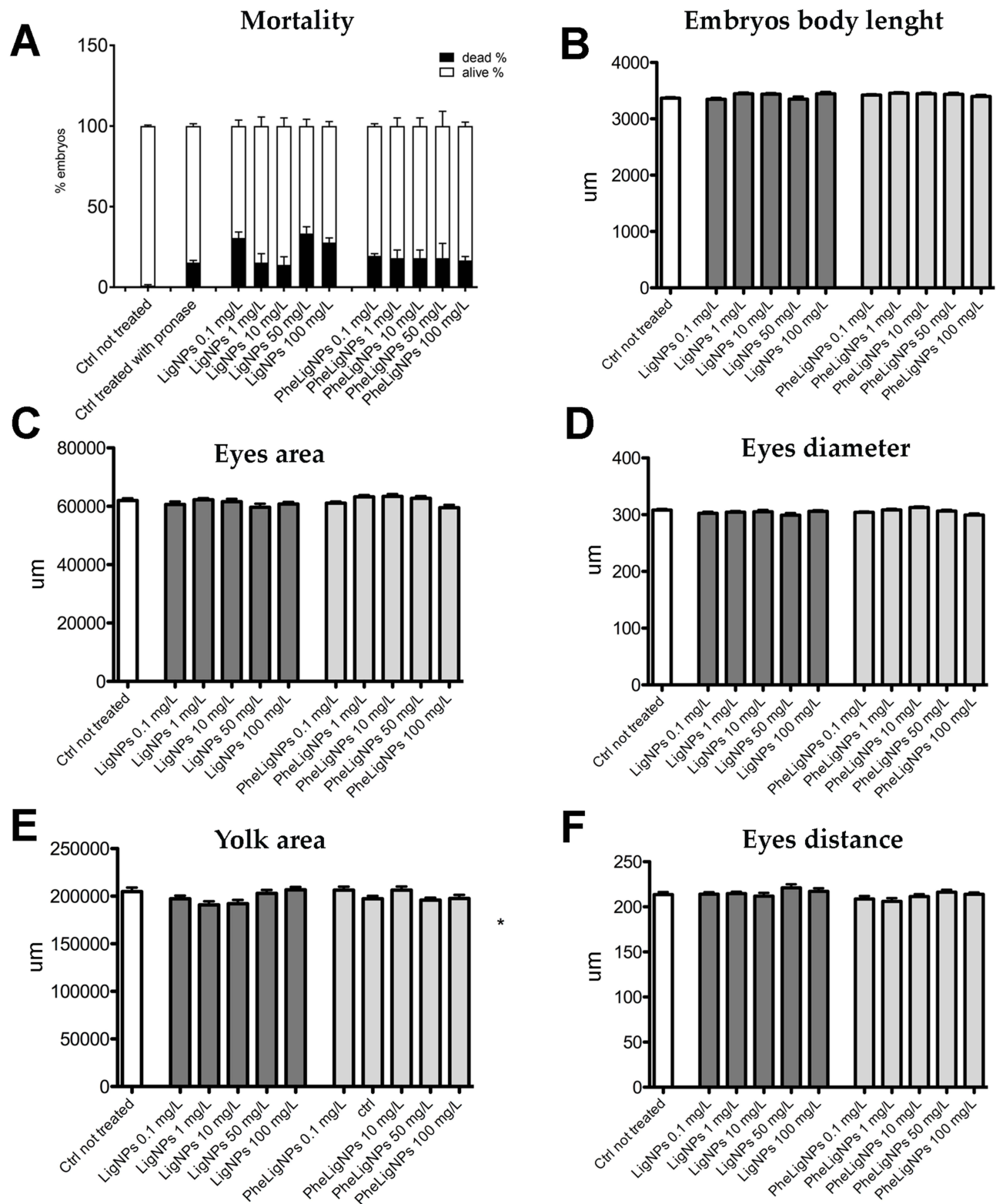


**Figure 3 (A)** Mortality reported as percentage after chemical pronase treatment. **(B-F)** Measures were performed on embryos at 96 hpf after exposure to both LigNPs and PheLigNPs at different concentrations. The analyses were taken on embryo body length, eye area and diameter, yolk area, and eye distance.

## Acute Inflammation Induced by *P. Aeruginosa* Lipopolysaccharide (LPS) Injection and Investigation of LigNPs and PheLigNPs Exposure Effects

The LPS is an inflammation inducer that stimulates the immune system cells that recognize it. To generate the first acute inflammation model, zebrafish embryos at the 30 hpf developmental stage were injected with 250 µg/mL of *P. aeruginosa* LPS (LPS). The chosen injection site was the apical part of the yolk. This particular site was selected to reduce possible damage to the embryo given by the injection itself and to take advantage of the natural yolk reabsorption, besides the proximity to the circulatory system.

Soon after the LPS injection, the embryos were exposed for 48 h to the LigNPs and PheLigNPs, at a concentration of 100 mg/L, as reported in the Material and Methods section. Successively, the RNA of these embryos was extracted and used for qRT-PCR analyses to observe the variation of gene expression levels related to inflammation. The genes observed were *tnfa*, *nfk2*, *il8*, *il6*, *il1β*, *nfkbiaa*, *ccl34a.4* (Figure 4). *Tnfa* is related to the immune system and the inflammatory response activation.<sup>35</sup> The *nfk2* is part of a complex that activates genes involved in inflammation and immune function, increasing the expression of pro-inflammatory molecules like *tnfa*, *il8*, *il6*, *il1β*.<sup>36</sup> *Nfkbiaa* is estimated to enable NF-kappa B binding activity, acting upstream of or within negative regulation of hematopoietic progenitor cell differentiation. Importantly, it is upregulated in repairing epithelium after injuries.<sup>37</sup> *Ccl34a.4* is a chemokine, named Chemokine ligand 34a, important for the zebrafish immune response.<sup>38</sup>

The results observed (Figure 4A) showed that *tnfa* expression levels increased in LPS-injected embryos and LPS-injected embryos treated both with LigNPs or PheLigNPs, compared to the negative control (Ctrl). Even if a descendant trend was visible in LPS-injected embryos exposed to LigNPs and to PheLigNPs, compared to positive control (LPS-injected embryos), the decrease was not statistically significant. The observation of the other gene expression levels (*nfk2*, *il8*, *il6*, *il1β*, *nfkbiaa*, and *ccl34a.4*) showed a similar tendency, meaning an increase in embryos LPS-LigNPs, compared to positive control (LPS injected embryos), and a decreasing trend in embryos LPS-PheLigNPs compared to embryos LPS-LigNPs, but not to positive control. The gene expression levels observed in embryos not LPS-injected and exposed to LigNPs and PheLigNPs are most of the time comparable or downregulated if compared to the negative or positive control embryos. These results, reported in Figure 4, (Figure 4B) and in [Additional Table 2](#), underline the absence of effects related to exposure to the studied NPs, highlighting their safety.

## Acute Inflammation Induced by Wound Injury and Evaluation of LigNPs and PheLigNPs Exposure Effects

Acute inflammation can be induced by tail wounding in zebrafish, a well-established model for inflammation and regeneration studies. Tail wounding was performed by incision of the zebrafish embryo fin with a sterile needle under a stereo microscope.<sup>39</sup>

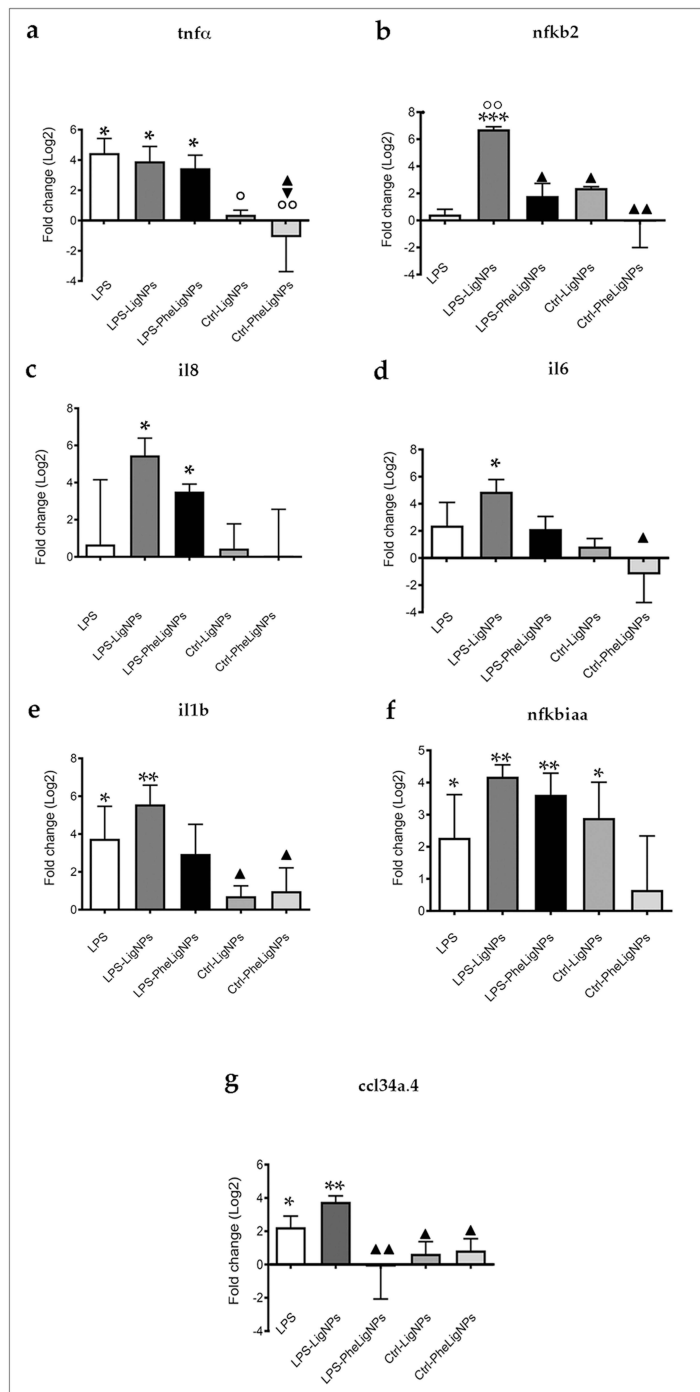
After the wound, the gene expression panel examined was the same as observed in embryos after LPS-induced inflammation (*tnfa*, *nfk2*, *il8*, *il6*, *il1β*, *nfkbiaa*, and *ccl34a.4*). For this inflammatory model, we observed an increase in almost all gene expression levels compared to the negative control (Ctrl not wounded), confirming its generation (Figure 4B). The results obtained showed an increase in *tnfa*, *il1β*, and *il6* expression levels in wounded and exposed to LigNPs or PheLigNPs embryos, compared to the positive control (Ctrl wounded) (Figure 4B, a, e and d). The *nfkbiaa* expression levels increased in wounded embryos exposed to LigNPs, but not to PheLigNPs, compared to positive control (Figure 4B, f). About *il8* expression levels, a significant decrease was observed in embryos wounded and exposed to both LigNPs and PheLigNPs, compared to positive control. The *ccl34a.4* expression level decreased only in wounded and exposed to PheLigNPs embryos, compared to positive control (Figure 4B, g). All results are reported in [Additional Table 3](#).

## The Neutrophil Number is Increased in Embryos Wounded and in Embryos Wounded and Exposed to LigNPs and PheLigNPs

An acute local inflammatory response can be observed in zebrafish embryos. In fact, an induced accumulation of neutrophils can be observed near the wounded area (Figure 5A). The zebrafish immune system is highly like that of

**A**

**LPS injection**



**B**

**Wound injury**

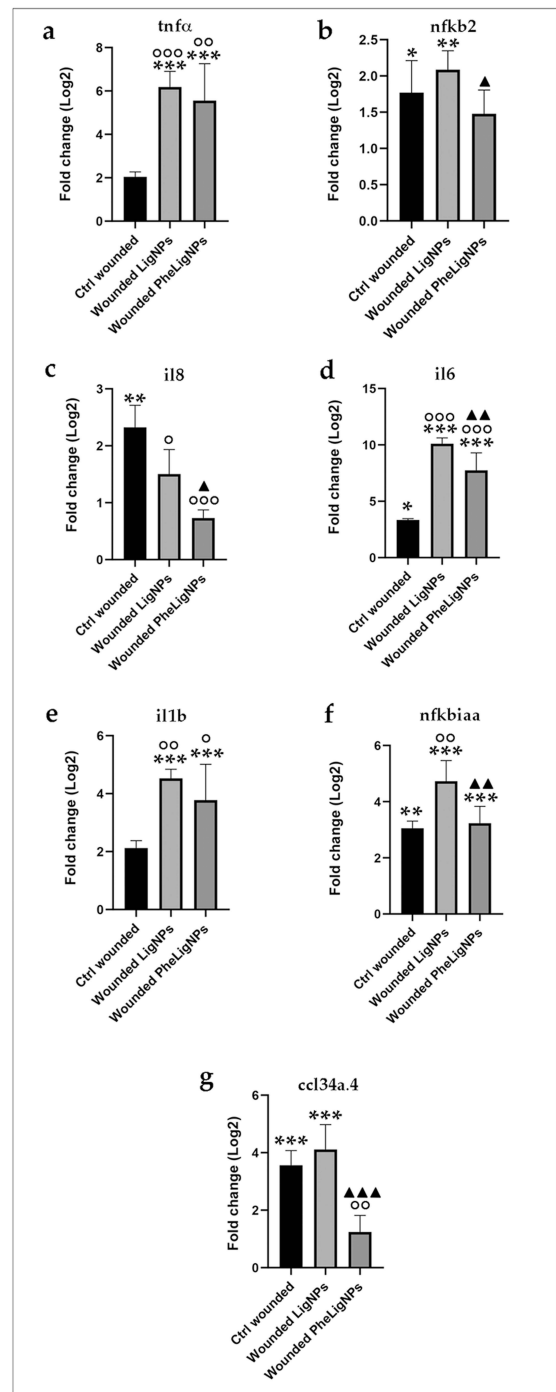


**Figure 4 (A).** Graphs reporting gene expression levels of *tnfa*, *nfkb2*, *il8*, *il6*, *il1b*, *nfkb1a*, and *ccl34a.4* in the acute inflammation model generated by *Pseudomonas aeruginosa* lipo-poly-saccharide (LPS) injection (250 µg/mL) in embryos at 30 hpf. The injected embryos were exposed soon after with LigNPs and PheLigNPs (100 mg/L), and compared to embryos not injected (Ctrl) or control embryos not injected but exposed to LigNPs or PheLigNPs. \*  $p < 0.05$  with respect to Ctrl; °  $p < 0.05$  with respect to LPS; ▲  $p < 0.05$  with respect to LPS-LigNPs; ▼  $p < 0.05$  with respect to LPS-PheLigNPs; \*\*  $p < 0.01$  with respect to Ctrl; °°  $p < 0.01$  with respect to LPS; ▲▲  $p < 0.01$  with respect to LPS-LigNPs \*\*\*  $p < 0.005$  with respect to Ctrl; **(B)** Graphs reporting the expression levels of the same genes observed in **(A)**, but on acute inflammation model obtained by wound. In this case, the wounded embryos exposed to LigNPs and PheLigNPs were compared to Ctrl wounded or Ctrl not wounded. \*  $p < 0.05$  with respect to Ctrl not wounded; °  $p < 0.05$  with respect to Ctrl wounded; ▲  $p < 0.05$  with respect to Wounded LigNPs; \*\*  $p < 0.01$  with respect to Ctrl not wounded; °°  $p < 0.01$  with respect to Ctrl wounded; ▲▲  $p < 0.01$  with respect to Wounded LigNPs; \*\*\*  $p < 0.005$  with respect to Ctrl not wounded; °°°  $p < 0.005$  with respect to Ctrl wounded; ▲▲▲  $p < 0.005$  with respect to Wounded LigNPs.

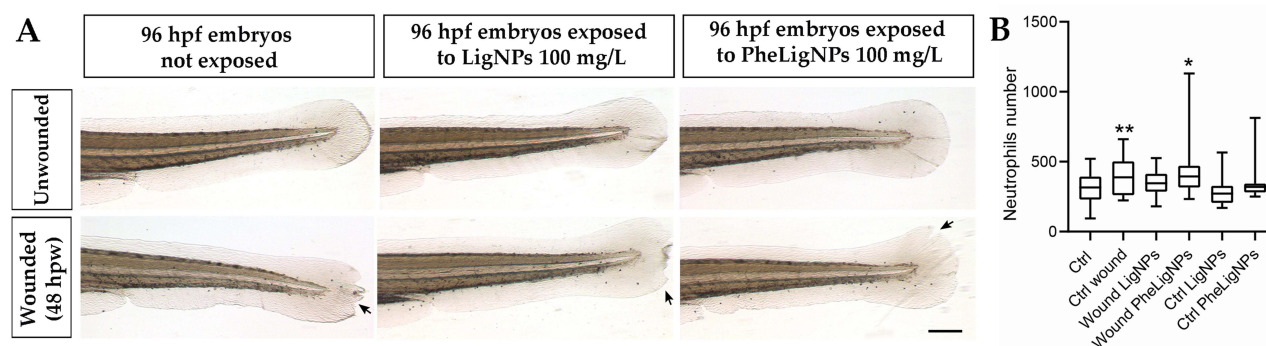


**Figure 5 (A).** Representative images wounding experiment. The number of neutrophils recruited in the caudal fin region, at the wound site, was observed and analyzed by Imagej (Fiji) software. **(B)** Data represents the mean  $\pm$  SEM of 3 independent experiments. Scale bar: 50  $\mu$ m. \*  $p < 0.05$  with respect to Ctrl not wounded; \*\*  $p < 0.01$  with respect to Ctrl not wounded.

humans, even if the first that matures during zebrafish development is the innate immune system. Macrophages, which can be observed from 15 hpf, are capable of phagocytosing particles, producing reactive oxygen species (ROS), and killing pathogens still during the onset of blood circulation at 26 hpf.<sup>40,41</sup> The zebrafish neutrophils, which develop by 18 hpf and mature between 24 and 48 hpf, resemble human neutrophils in terms of the presence of segmented nuclei, cytoplasmic granules, and expression of myeloperoxidase.<sup>42</sup>

It is important to know that the embryonic tail fin is not a vascularized tissue and that many of the recruited neutrophils migrate to the wound from nearby tissues, such as the CHT.<sup>39</sup>

To observe if lignin NPs could have a role in the neutrophils' recruitment, we caused an injury to 48 hpf embryos and exposed them to LigNPs and PheLigNPs at the concentration of 100 mg/L, the highest concentration used in this work, for 72 h. Thereafter, Sudan black b staining was used to mark the mature neutrophils. The results showed a significant increase in neutrophils number in the positive control embryos (Ctrl wounded), and in embryos wounded and exposed to PheLigNPs, compared to negative control (embryos not wounded - Ctrl). Upregulation of neutrophils was observed also in the wounded embryos exposed to LigNPs, though not significant, while in embryos not wounded and exposed to LigNPs and PheLigNPs, the increased neutrophils number was negligible, again confirming the absence of effects towards these NPs (Figure 5B).

## LigNPs and PheLigNPs Inhibit the Canonical Wnt/ $\beta$ -Catenin Pathway

Zebrafish embryos are an emerging organism to study the cutaneous wound healing, particularly in the field of drug discovery. In this model, the wound-healing progression recapitulates the stages observed in mammals, except for the blood-clotting phase. The other processes, such as inflammation, re-epithelialization, granulation tissue formation, and, finally, remodeling, are resulting very similar.<sup>43</sup>

In this scenario, the canonical Wnt signaling pathway plays diverse and important roles during regeneration of different organisms. In the zebrafish fin regeneration, the blastema, which is an organized mass of tissue characterized by the presence of stem/progenitor cells, is the principal actor that manages the mesenchymal regenerative process. The Wnt pathway is activated during blastema formation in a spatiotemporal regulated manner, playing a role in tissue organization and differentiation, besides in the proliferation of the blastema cells. In mammals, the *Wnt/ $\beta$ -catenin* pathway activity is maintained in the adult organism only in specific organs/tissues with high cell turnover, such as the epidermis.<sup>44</sup>

Taking into consideration the different properties that lignin NPs presented, we decided to evaluate if LigNPs and PheLigNPs could have effects on the wound healing process in embryos exposed (Figure 6), at the molecular level (Figure 6). The results obtained showed that the embryos wounded and exposed to 100 mg/L LigNPs and PheLigNPs, presented a significantly decreased level of *wnt4a*,  $\beta$ -catenin, and *gsk3 $\beta$* , with PheLigNPs showing the higher (although not significant) capacity to downregulate these genes. About the *wnt10b* expression level, a significant decrease was observed only after PheLigNPs exposure, compared to positive control, whereas increased levels were observed after



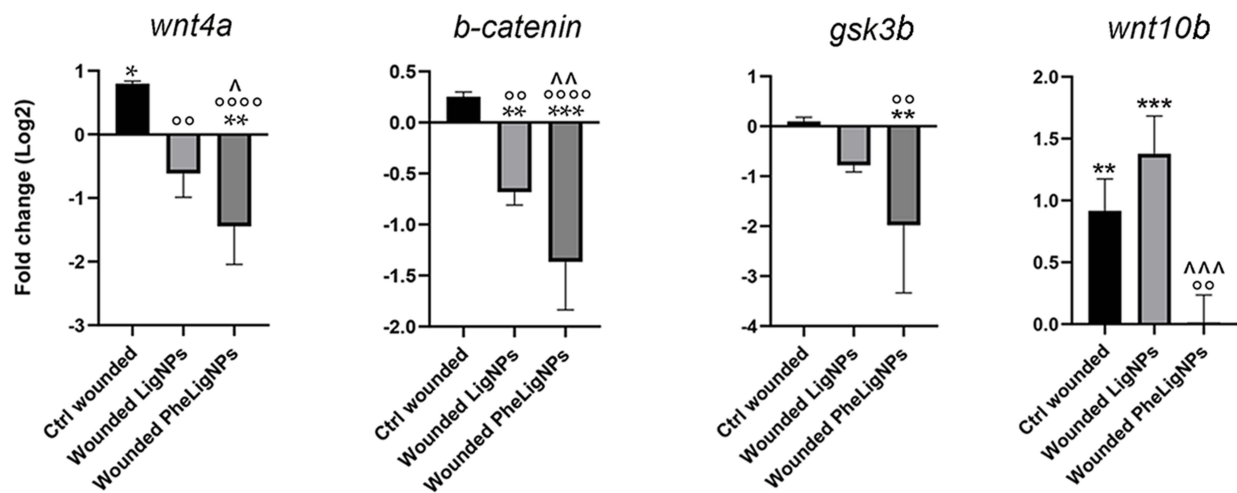
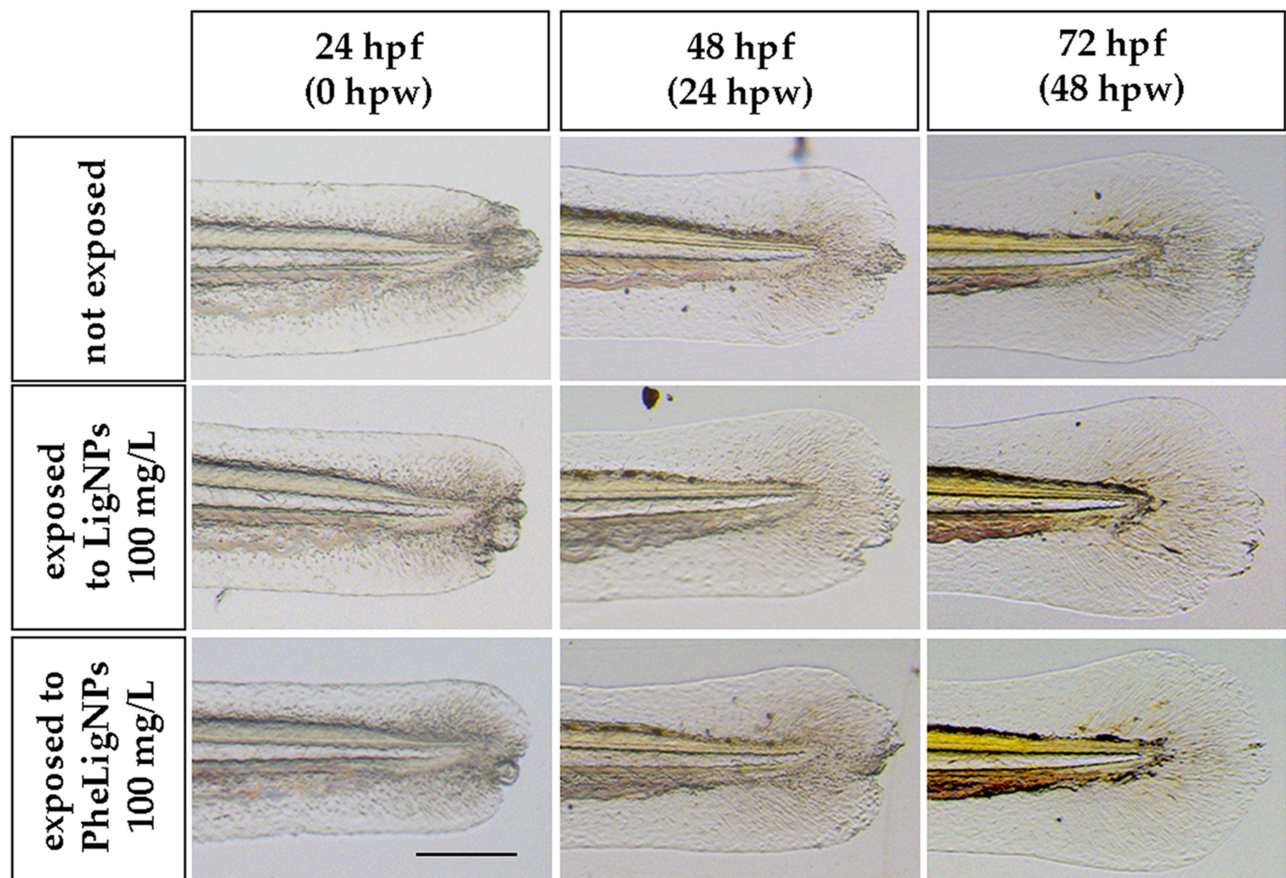


**Figure 6** Representative images of wound injury provoked in embryos at 48 hpf. The wounded embryos were soon after treated with lignin nanoparticles, and compared with Ctrl wounded and Ctrl not wounded embryos till the 96 hpf developmental stage. Successively, *wnt4a*, *β-catenin*, *gsk3β*, and *wnt10b* expression levels were evaluated by qPCR in each experimental group. The genes observed are related to the *Wnt/β-catenin* signaling pathway, fundamental for the regeneration process. Scale bar: 50 μm. \*  $p < 0.05$  with respect to Ctrl not wounded; <sup>^</sup>  $p < 0.05$  with respect to Wounded LigNPs; \*\*  $p < 0.005$  with respect to Ctrl not wounded; <sup>^^</sup>  $p < 0.005$  with respect to Ctrl wounded; <sup>^^^</sup>  $p < 0.005$  with respect to Wounded LigNPs; \*\*\*  $p < 0.01$  with respect to Ctrl not wounded; <sup>^^^</sup>  $p < 0.01$  with respect to Wounded LigNPs; <sup>^^^^</sup>  $p < 0.001$  with respect to Ctrl wounded.

LigNPs, compared to negative control, but not to positive control (Figure 6 Additional Table 4). As shown in the upper panel of Figure 6 (Figure 6), a better regeneration process of the zebrafish caudal fin is visible in embryos exposed to lignin NPs after wound injury.

## Discussion

NPs derived from renewable resources, such as biomass, and thus called bio-based NPs (B-NPs), are nano-formulated particles with multiple functionalities, such as antimicrobial, antioxidant, and UV-blocking properties. B-NPs, besides their application in several sectors, including packaging, construction, and automotive industries, are also raising an increased interest in other fields, such as medicine and therapeutics. The use of natural bio-based NPs and bio-polyols is a novel strategy that producers identified for the generation of not-harmful greener nano-formulations that consider the development of engineered particles by using renewable or biomass-derived resources. The broad application potential of these B-NPs will valorize biomass wastes in safe and sustainable for the environment and human uses. From such a perspective, the natural polyphenolic compounds from lignocellulose biomass, namely lignins and tannins, feature a myriad of intrinsic properties derived from their composition like antioxidant activity, anti-inflammatory activity, and stacking tendencies.<sup>45</sup>

In this work, we wanted to explore the anti-inflammatory potential of sono-enzymatically synthesized nanoparticles from pristine (LigNPs) and phenolated with TA and GA for increased reactivity lignin (PheLigNPs).<sup>6,7</sup> Data from physicochemical characterization, performed in both mQ water and FET medium and at different time points, confirmed the colloidal stability of LigNPs and PheLigNPs, the presence of different population sizes, and their midrange mono-dispersion in the medium used. LigNPs and PheLigNPs were negatively charged in mQ, while in FET medium presented a reduced negative charge, probably due to the ionic and salt composition of this solution.

To evaluate in depth the direct interaction of LigNPs and PheLigNPs with the zebrafish embryos, we relied on a test to evaluate toxicity on zebrafish embryos chorion deprived, according to the guidelines of the ISO/TS 22082:2020 Nanotechnologies — Assessment of nanomaterial toxicity using dechorionated zebrafish embryo. Since the chorion is a natural barrier that protects the embryo from external influences, its removal facilitates a toxicological assessment that is more indicative of direct exposure to NPs or nanomaterials (NMs). The OECD test guideline using fish embryos to evaluate acute toxicity (see OECD TG 236) is reporting that this classic test might be inappropriate for assessing substances characterized by a molecular weight  $\geq 3$  kDa, or a cumbersome molecular structure, or known to be the cause of a delayed hatching in embryos. Moreover, the presence of the chorion can affect the results of the nanomaterials' biological activity.

The use of this test is not directly intended for retrieving toxicological information but will help to better identify potentially hazardous NMs. There are two ways to remove the chorion from embryos during early developmental stages (6–8 hpf), an enzymatic method and a mechanical method. The enzymatic method presents some advantages, such as time and labor efficiency by easy preparation for dechorionation, no mechanical embryonic damage, and the possibility to prepare a large number of dechorionated embryos for a high throughput-based approach at the same time. On the other hand, there is a disadvantage of variability in pronase activity that could influence the success rate of chorion removal.

The pronase treatment was performed on embryos at 6 hpf using an enzyme mixture of several non-specific endoproteases and exoproteases from *Streptomyces griseus*. At 24 hours post-treatment (hpt), we observed a mortality rate of about 27%, which is a percentage compliant with reports on the same treatment.<sup>34</sup> The mortality observed at 96 hours, the end of the exposure period with different concentrations of LigNPs and PheLigNPs, was paltry and not attributable to an effect of the NPs exposure. For instance, it is reported that polyphenols show anti-inflammatory capabilities, largely due to the antioxidant activity of the phenolic groups. In different conditions, characterized by an inflammatory state, oxidative stress produces an excess of reactive oxygen species (ROS) in damaged cells and tissues. The antioxidant capacity of polyphenols lies in their ability to suppress the formation of ROS, inhibiting the activity of many enzymes involved in their production, or stimulating the synthesis of antioxidant defenses.<sup>46–49</sup>

Furthermore, the embryos fixed at 96 hpf after exposure to the NPs, were evaluated for morphological parameters possibly affected by the NMs used. Body length, eye distance, area, and diameter, besides the yolk sac area, did not show differences, after any concentration used, compared to control embryos at the same developmental stage. To date, the highest concentration (100 mg/L) used for the experimental analyses is greater than the lignin NPs concentration reported in literature, tested for biomedical purposes.<sup>25</sup>

Considering the safety of lignin NPs highlighted by the results obtained, and the lack of acute developmental toxicity, besides the possible applications that LigNPs and PheLigNPs may find as antimicrobial agents for biomedical purposes,<sup>50</sup>

we investigated whether these NPs could be able to modulate the immune response, possibly showing anti-inflammatory characteristics. Therefore, we tested LigNPs and PheLigNPs on two different inflammatory models generated in zebrafish embryos - one obtained by the injection of lipopolysaccharide from *P. aeruginosa* (LPS), and the other by wounding the caudal fin.

To generate the first inflammatory model, we injected the LPS at a concentration of 250 µg/mL / embryo. In the zebrafish model, the LPS-induced inflammation is generally established by non-invasive immersion of embryos in a growth medium containing LPS<sup>51,52</sup> or injection into the yolk.<sup>10</sup> In our case, the site chosen for inoculation was the upper part of the yolk sac of embryos at 30 hpf, to avoid the eventual LPS sequestration by the bio-based nanomaterial (NM) used. The LPS concentration of 250 µg/mL was selected to obtain an acute inflammation without causing death, since it is half of the concentration generally injected to cause acute fatal inflammation (500 µg/mL).<sup>10</sup> After the LPS injection, we left the embryos at 27±1 °C for 18 h and when the embryos (LPS-injected or not) reached the 48 hpf developmental stage, we exposed them to the LigNPs and PheLigNPs for 72 h. Thereafter we observed the expression levels of the following inflammation-related genes: *tnfa*, *nfkb2*, *il8*, *il6*, *il1β*, *nfkb1a*, and *ccl34a.4*.

The increased level of the majority of genes observed in LPS-injected embryos (positive control), and LPS-injected embryos exposed to LigNPs and PheLigNPs, compared to the controls not injected (negative control), highlight the fact that, despite the low level of LPS inoculated in embryos (1 nL/embryo of 250 µg/mL LPS), we were able to establish our first inflammatory model. Interestingly, we observed a significant increase in *nfkb2* expression level in LPS-injected embryos exposed to LigNPs, but not to PheLigNPs, compared to LPS-injected embryos (our positive control). *Nfkb2* is a gene that encodes two members of the NF-κB/Rel family of proteins, that regulate an array of target genes involved in the immune, antiapoptotic, acute-phase responses and inflammatory processes.<sup>53</sup>

We hypothesize that LigNPs could increase intracellular oxidation. This fact can be related to the sonochemical production of the NPs,<sup>6</sup> where hydrogen peroxide may be generated.<sup>54</sup> This oxidative agent is known to cause oxidative damage/stress in cellular models<sup>55</sup> and.<sup>56</sup> However, we did not observe the same effect with sonochemically nanoformulated PheLigNPs, probably due to the increased phenolic content of these NPs endowing them with high antioxidant capacity to mitigate possible peroxide activity. The expression levels of *tnfa*, *il8*, *il6*, *il1β*, *nfkb1a*, and *ccl34a.4* showed an increased trend, if compared to positive control, even though this is not statistically significant. It can be appreciated in this case again, the fact that the increase is more visible after LigNPs than PheLigNPs exposure.

Moreover, the increased trend observed among the inflammatory pathway genes can be related to a normal upregulation of the innate immune system, characterizing the embryos at the developmental stage in which they were analyzed, in response to exogenous stimuli.<sup>57</sup> The only effect that we observed in embryos not injected and exposed to NPs, was related to the increased *nfkb1a* expression level after exposure to LigNPs. Since *nfkb1a* is a *nfkb2* target gene, it is expected that it will show similar behavior in embryos exposed to LigNPs, compared to the negative control. In summary, a general increasing trend in inflammatory gene expression levels in LPS-injected embryos after exposure to LigNPs, in comparison to LPS-injected embryos exposed to PheLigNPs, was detected. This result highlighted the potential for biomedical applications of the functionalized lignin NPs, which combine the known positive characteristic of polyphenols,<sup>58,59</sup> with the power of tannins<sup>60,61</sup> in the same nano-entity.

The second inflammatory model was generated by performing a wound injury in the terminal portion of the caudal fin in zebrafish embryos at 48 hpf. The wound was not the classical fin-clip, but a minor damage of the epidermis, to mimic a scratch rather than a cut. The wounded embryos were immediately exposed to both NPs for 72 h, and analyzed at the molecular level at 96 hpf for the same inflammatory genes studied in the LPS model. We observed a generalized increase in expression levels of inflammatory genes in wounded embryos, exposed or not to both NPs, if compared with the negative Control (not wounded embryos). These results confirmed that we were able to generate an inflammatory model.

The data obtained comparing the wounded embryos exposed to both NPs to wounded embryos not exposed (positive Control) showed significantly increased expression levels in *tnfa*, *il6*, *il1β*, *ccl34a.4*, and *nfkb1a*. The results obtained are in line with the report of Xie et al, who observed the same gene levels increased after wounding.<sup>39</sup> To date, the NF-κB activation, which can be related to the significant increase of *nfkb1a* expression level and the increased trend in *nfkb2* levels in our research, was shown to be dependent on the phosphorylation of the extracellular signal-regulated kinases (ERKs), which results in an increased expression of pro-inflammatory molecules like *tnfa*, *il1β*, *il6*, and *il8* upon tail



wounding. This upregulation mediates neutrophil recruitment through *Cxcr2*, an intermediary of the neutrophils' promigratory pathway.<sup>62</sup> Importantly, *tnfa*, *il1 $\beta$* , and *ccl34a.4* are recognized wound-healing markers,<sup>63</sup> and the aforementioned intracellular nuclear factor-kB (NF-kB) is not exclusively a mediator of the pro-inflammatory response, but in parallel, it is known to activate the nuclear factor NRF2, which in turn is responsible for the anti-inflammatory response.<sup>64</sup>

Finally, we observed increased *il6* levels. This could be explained by the fact that interleukin-6 is known to be produced in response to tissue injuries, given the case that it contributes to host defense through the stimulation of acute phase responses, hematopoiesis, and immune reactions.<sup>65</sup> We detected only two genes, *il8* and *ccl34a.4*, that were significantly downregulated after exposure of wounded embryos to PheLigNPs. As we reported for LPS-injected embryos exposed to LigNPs, also in this wound model we observed a general trend of increased expression levels of inflammatory genes after exposure to LigNPs, while, interestingly, after the PheLigNPs exposure a reduction of the genes' expression level is observed. We are firmly convinced that this is a further demonstration of the beneficial effect of the presence of tannins in the functionalized NPs.

Moreover, it is known that cytokines such as *tnfa* and *il1 $\beta$*  are important for cutaneous homeostasis maintenance, and alteration in the transcriptional levels of these molecules is a characteristic feature of the immune response, for example, to sunburn, which can be considered an epidermis damage comparable to the injury that we provoked in the embryos' fin.<sup>66,67</sup> About this point, Banerjee and Leptin's research highlighted that, despite the role of *il1 $\beta$*  as a potent proinflammatory cytokine involved in acute inflammatory response to several conditions, it is characterized also by the less well-known role as a mediator in tissue repair and reconstitution. This aspect was studied in a UV-exposure zebrafish model, in which the researchers demonstrated the protective role of *il1 $\beta$* , showing that higher levels of *il1 $\beta$*  correspond to better survival rates post-UV exposure.<sup>68</sup> This type of damage can be compared to the injury that we inflicted on the embryos' caudal fin, which was superficial and did not harm the blastema. Therefore, we hypothesize that the *il1 $\beta$*  increased levels observed by qPCR can be reconducted to the incipit of its protective action. Based on the aforementioned observations and on the fact that the increased expression gene levels were observed in embryos wounded and exposed to both LigNPs and PheLigNPs, we can conclude that these NPs demonstrated to have a beneficial role during wound healing in zebrafish embryos.

To further evaluate the effect of LigNPs and PheLigNPs exposure, and to confirm that the increased inflammatory gene levels were not related to proinflammatory activity of the NPs, we monitored the neutrophils recruitment at the injury site by Sudan black B staining. Neutrophils are one of the major components of the innate immune response, besides to be the most abundant circulating cell type in humans and zebrafish.<sup>69</sup> The Sudan black (SB) is a mature neutrophil marker. The first mature SB-positive neutrophils can be detected from 35 hpf, even if the entire fully mature neutrophils are present by 48 hpf, under steady-state conditions.<sup>70</sup> By the use of this staining, we could detect if there would be an increase in neutrophils' number in wounded embryos exposed to LigNPs and PheLigNPs, not only at the injury spot but also at the Caudal Hematopoietic Tissue (CHT), the region for neutrophil production during larval development (similar to the mammalian fetal liver).

We observed a significant increase in neutrophil number after wounding, compared to the negative control, highlighting the fact that we were able to generate an inflammatory model by harming superficially the embryos' fin. After 48 hours of exposure to both LigNPs and PheLigNPs at the highest concentration, the wounded embryos did not show any significant neutrophil number increase, compared to the positive control (wounded embryos). This result demonstrates that at tissue level, the lignin NPs do not increment the acute inflammation episode, caused by the wound.

The last experiment performed was to evaluate if the LigNPs and PheLigNPs could have a beneficial action on cutaneous homeostasis maintenance, given the fact that these NPs increased expression levels of *tnfa*, *il1 $\beta$* , *il6*, and *ccl34a.4*. In this case, we observed the healing of the fin injury and evaluated the *Wnt/ $\beta$ -catenin* signaling, which is necessary for normal progression of the injury response during regeneration. Moreover, this pathway regulates macrophage chemotaxis, recruitment, and inflammatory diseases in several organisms, besides being a candidate for linking inflammation and regeneration in zebrafish.<sup>71</sup> Petrie et al reported that *Wnt/ $\beta$ -catenin* signaling is required not only for regenerative outgrowth in zebrafish caudal fins but also modulates inflammatory processes including scar formation, fibrosis, wound healing, and tissue remodeling in mammals.<sup>71</sup> Based on this, we attempted to analyze the expression



levels of *wnt4a*,  $\beta$ -catenin, *gsk3 $\beta$* , and *wnt10b*, related to the *Wnt*/ $\beta$ -catenin signaling pathway, in wounded embryos, exposed or not to both lignin NPs. Our data showed that the exposure to LigNPs significantly downregulated the expression level of *wnt4a*,  $\beta$ -catenin, and *gsk3 $\beta$* , but not *wnt10b*. The latter is increased compared to the negative control (not wounded embryos), but not to the positive control (wounded embryos). Conversely, the exposure to PheLigNPs reduced the expression levels of every gene observed, compared to the positive control.

The *Wnt*/ $\beta$ -catenin signaling pathway plays fundamental roles in many biological processes including neurodevelopment, cell survival, and cell cycle regulation, besides in embryonic development.<sup>72</sup> Bastakoty et al realized that the modulation in *Wnt* signals during regeneration and tissue repairing processes can have a positive effect.<sup>44,73</sup> For instance, they reported that in the dermis, the *Wnt* inhibition promoted granulation tissue resolution and deposition of a more organized extracellular matrix, indicating a better restoration of the dermal-epidermal junction (35). We hypothesize that the *Wnt*/ $\beta$ -catenin repression observed after LigNPs exposure, and even more, after PheLigNPs exposure, can have beneficial effects on embryos' caudal fin wound injury. The differences observed in *Wnt* modulation between the two NPs can be ascribed to the increased number of phenolic groups on lignin due to enzymatic grafting of the phenolic compounds. The tannic acids, a generic term for hydrolysable tannins, are characterized by the presence of various phenol groups. They are known to prevent photo-damage and photoaging by inhibiting oxidation levels and to protect the human skin from UV radiation. Furthermore, they are reported to mitigate the oxidative stress and modulate the activity of pro-inflammatory enzymes, such as cyclooxygenases (COX) and lipooxygenases (LOX), in the extracellular space, while reducing the binding of pro-inflammatory cytokines to receptors in the cellular membrane<sup>74–76</sup> and to have a scarring effect in wound repair.<sup>77</sup>

## Conclusion

In this study, the sono-enzymatically functionalized and nanoformulated lignin NPs showed interesting bioactivities, beyond their antibacterial, antioxidant and anti-UV features. The lignin NPs did not affect zebrafish development and did not significantly trigger an acute inflammation episode, indicating the safety of these bio-based nanomaterials and their functionalization/nanotransformation methods. We observed an increase in inflammatory gene expression levels in inflammatory models generated in zebrafish embryos after exposure to LigNPs and PheLigNPs. We hypothesize that both NPs could have a positive role in inflammatory event resolution, recalling cytokines and chemokines to resolve the damage. Moreover, the increased expression levels of some genes, such as *il1 $\beta$*  or *il6* and *tnfa*, can be related to a favorable healing process, based on increased tissue regeneration and scarring, as also confirmed by the effective modulation of the *Wnt*/ $\beta$ -catenin expression pattern.

Even if we do not observe clear anti-inflammatory properties of LigNPs and PheLigNPs, we can confirm that these lignin-based NPs showed the capacity to induce a positive response in an inflammatory event, increasing the recruitment of cytokines to accelerate their chemotactic function. Moreover, the LigNPs and PheLigNPs can also have a role in the resolution of wounds, favoring the regeneration process.

The nanoformulated lignin certainly requires additional investigation as a bioactive material, not only because safe enzymatic and nanotransformation processes can efficiently modulate its biological activity and safety profile, but also because of its potential for biomedical purposes.

For example, the comparison with additional NPs of other or similar nature (organic, inorganic, persistent or more soluble) can be helpful to confirm beyond doubt the specificity of the effects observed with LigNPs and PheLigNPs.

Moreover, we are aware that further toxicity studies, scalability of nanoparticle production, and regulatory approvals will be necessary before the wide application of lignin nanoparticles and its modifications in the medical field, but the potentialities in terms of biocompatibility, intrinsic powerful properties, and availability of this natural material will surely deserve the effort.

## Abbreviations

NPs, nanoparticles; hpf, hours post fertilization; LigNPs, lignin nanoparticles; PheLigNPs, phenolated lignin nanoparticles; FET, fish embryo medium; mQ, milliQ water; NM, nanomaterials; LPS, lipopolysaccharide from *Pseudomonas Aeruginosa*; SB, Sudan Black B; CHT, Caudal Hematopoietic Tissue; B-NPs, bio-based nanoparticles.

## Data Sharing Statement

The datasets supporting the conclusions of this article are included within the article (and its [additional tables](#)). The data that support the findings of this study are available from the corresponding author upon reasonable request.

## Acknowledgments

The authors thank Dr. Saibene Melissa (Microscopy facility, University of Milano-Bicocca, Piazza della Scienza 3, 20126 Milano, Italy) for the TEM images. Support for the research of T.T was also received through the prize “ICREA Academia” for excellence in research funded by the Generalitat de Catalunya.

## Author Contributions

All authors made a significant contribution to the work reported, whether that is in the conception, study design, execution, acquisition of data, analysis and interpretation, or in all these areas; took part in drafting, revising or critically reviewing the article; gave final approval of the version to be published; have agreed on the journal to which the article has been submitted; and agree to be accountable for all aspects of the work.

## Funding

This research was performed within the EU-H2020 project BIOMAT, funded by the European Union’s Horizon 2020 research and innovation program under grant agreement No 953270.

## Disclosure

The authors report no conflicts of interest in this work.

## References

1. Ragauskas AJ, Beckham GT, Bidy MJ, et al. Lignin valorization: improving lignin processing in the biorefinery. *Science*. 2014;344(6185):1246843. doi:10.1126/science.1246843
2. Upton BM, Kasko AM. Strategies for the conversion of lignin to high-value polymeric materials: review and perspective. *Chem Rev*. 2016;116(4):2275–2306. doi:10.1021/acs.chemrev.5b00345
3. Wang R, Zheng L, Xu Q, et al. Unveiling the structural properties of water-soluble lignin from gramineous biomass by autohydrolysis and its functionality as a bioactivator (anti-inflammatory and antioxidative). *Int J Biol Macromol*. 2021;191:1087–1fv095. doi:10.1016/j.ijbiomac.2021.09.124
4. Zeb A. Concept, mechanism, and applications of phenolic antioxidants in foods. *J Food Biochem*. 2020;44(9):1–22. doi:10.1111/jfbc.13394
5. Qian Y, Zhong X, Li Y, Qiu X. Fabrication of uniform lignin colloidal spheres for developing natural broad-spectrum sunscreens with high sun protection factor. *Ind Crops Prod*. 2017;101:54–60. doi:10.1016/j.indcrop.2017.03.001
6. Pérez-Rafael S, Ferreres G, Kessler RW, et al. Continuous sonochemical nanotransformation of lignin – process design and control. *Ultrason Sonochem*. 2023;98. doi:10.1016/j.ultsonch.2023.106499.
7. Morena AG, Tzanov T. Antibacterial lignin-based nanoparticles and their use in composite materials. *Nanoscale Adv*. 2022;4(21):4447–4469. doi:10.1039/d2na00423b
8. Jiang P, Sheng X, Yu S, et al. Preparation and characterization of thermo-sensitive gel with phenolated alkali lignin. *Sci Rep*. 2018;8(1):14450. doi:10.1038/s41598-018-32672-z
9. Luo B, Jia Z, Jiang H, Wang S, Min D. Improving the reactivity of sugarcane bagasse Kraft lignin by a combination of fractionation and phenolation for phenol-formaldehyde adhesive applications. *Polymers*. 2020;12(8):1825. doi:10.3390/POLYM12081825
10. Yang LL, Wang GQ, Yang LM, Huang ZB, Zhang WQ, Yu LZ. Endotoxin molecule lipopolysaccharide-induced zebrafish inflammation model: a novel screening method for anti-inflammatory drugs. *Molecules*. 2014;19(2):2390–2409. doi:10.3390/molecules19022390
11. Yan B, Lu G, Wang R, et al. Protective effects of lignin fractions obtained from grape seeds against bisphenol AF neurotoxicity via antioxidative effects mediated by the Nrf2 pathway. *Front Chem Sci Eng*. 2023;17(7):976–989. doi:10.1007/s11705-022-2237-0
12. Wang B, Sun D, Wang HM, Yuan TQ, Sun RC. Green and facile preparation of regular lignin nanoparticles with high yield and their natural broad-spectrum sunscreens. *ACS Sustain Chem Eng*. 2019;7(2):2658–2666. doi:10.1021/acssuschemeng.8b05735
13. Zhou F, Wang M, Ju J, et al. Schizandrin protects against cerebral ischemia-reperfusion injury by suppressing inflammation and oxidative stress and regulating the AMPK/Nrf2 pathway regulation. *Am J Transl Res*. 2019;11(1):199–209.
14. Irvani S, Varma RS. Greener synthesis of lignin nanoparticles and their applications. *Green Chem*. 2020;22(3):612–636. doi:10.1039/c9gc02835h
15. Domínguez-Robles J, Cárcamo-Martínez Á, Stewart SA, Donnelly RF, Larrañeta E, Borrega M. Lignin for pharmaceutical and biomedical applications – could this become a reality? *Sustain Chem Pharm*. 2020;18. doi: 10.1016/j.scp.2020.100320.
16. Liu R, Dai L, Xu C, Wang K, Zheng C, Si C. Lignin-based micro- and nanomaterials and their composites in biomedical applications. *ChemSusChem*. 2020;13(17):4266–4283. doi:10.1002/cssc.202000783
17. Sugiarto S, Leow Y, Tan CL, Wang G, Kai D. How far is Lignin from being a biomedical material? *Bioact Mater*. 2022;8:71–94. doi:10.1016/j.bioactmat.2021.06.023

18. Nan N, Hu W, Wang J. Lignin-based porous biomaterials for medical and pharmaceutical applications. *Biomedicines*. 2022;10(4):1–16. doi:10.3390/biomedicines10040747
19. Prasad V, Siddiqui L, Mishra PK, Ekielski A, Talegaonkar S. Recent advancements in lignin valorization and biomedical applications: a patent review. *Recent Pat Nanotechnol*. 2021;16(2):107–127. doi:10.2174/1872210515666210216085831
20. Figueiredo P, Lintinen K, Kiriazis A, et al. In vitro evaluation of biodegradable lignin-based nanoparticles for drug delivery and enhanced antiproliferation effect in cancer cells. *Biomaterials*. 2017;121:97–108. doi:10.1016/j.biomaterials.2016.12.034
21. Phan NM, Nguyen TL, Shin H, Trinh TA, Kim J. ROS-scavenging lignin-based tolerogenic nanoparticle vaccine for treatment of multiple sclerosis. *ACS Nano*. 2023;17(24):24696–24709. doi:10.1021/acsnano.3c04497
22. Cassar S, Adatto I, Freeman JL, et al. Use of Zebrafish in drug discovery toxicology. *Chem Res Toxicol*. 2020;33(1):95–118. doi:10.1021/acs.chemrestox.9b00335
23. Howe K, Clark MD, Torroja CF, et al. The zebrafish reference genome sequence and its relationship to the human genome. *Nature*. 2013;496(7446):498–503. doi:10.1038/nature12111
24. Phillips JB, Westerfield M. Zebrafish models in translational research: tipping the scales toward advancements in human health. *DMM Dis Models Mech*. 2014;7(7):739–743. doi:10.1242/dmm.015545
25. Deng J, Gu J, Zhao X, et al. Improving the protective ability of lignin against vascular and neurological development in BPAF-induced zebrafish by high-pressure homogenization technology. *Int J Biol Macromol*. 2023;227:231. doi:10.1016/j.ijbiomac.2023.123356
26. Zandrea R, Bonan CD, Campos MM. Zebrafish as a model for inflammation and drug discovery. *Drug Discov Today*. 2020;25(12):2201–2211. doi:10.1016/j.drudis.2020.09.036
27. Russo I, Sartor E, Fagotto L, Colombo A, Tiso N, Alaibac M. The Zebrafish model in dermatology: an update for clinicians. *Discov Oncol*. 2022;13(1). doi:10.1007/s12672-022-00511-3
28. Kimmel CB, Ballard WW, Kimmel SR, Ullmann B, Schilling TF. Stages of embryonic development of the zebrafish. *Dev Dyn*. 1995;203(3):253–310. doi:10.1002/aja.1002030302
29. Le guyader D, Redd MJ, Colucci-Guyon E, et al. Origins and unconventional behavior of neutrophils in developing zebrafish. *Blood*. 2008;111(1):132–141. doi:10.1182/blood-2007-06-095398
30. Jiang B, Zhang Y, Gu L, Wu W, Zhao H, Jin Y. Structural elucidation and antioxidant activity of lignin isolated from rice straw and alkali-oxygen black liquor. *Int J Biol Macromol*. 2018;116:513–519. doi:10.1016/j.ijbiomac.2018.05.063
31. Schneider CA, Rasband WS, Eliceiri KW. NIH image to imageJ: 25 years of image analysis. *Nat Methods*. 2012;9(7):671–675. doi:10.1038/nmeth.2089
32. Shi Z, Xu G, Deng J, et al. Structural characterization of lignin from *D. sinicus* by FTIR and NMR techniques. *Green Chem Lett Rev*. 2019;12(3):235–243. doi:10.1080/17518253.2019.1627428
33. Garcia-Ubasart J, Colom JF, Vila C, Hernández NG, Blanca Roncero M, Vidal T. A new procedure for the hydrophobization of cellulose fibre using laccase and a hydrophobic phenolic compound. *Bioresour Technol*. 2012;112:341–344. doi:10.1016/j.biortech.2012.02.075
34. Martínez-Sales M, García-Ximénez F, Espinós F. Zebrafish (*Danio rerio*) as a possible bioindicator of epigenetic factors present in drinking water that may affect reproductive function: is chorion an issue? *Zygote*. 2014;23(3):447–452. doi:10.1017/S0967199414000045
35. van Loo G, Bertrand MJM. Death by TNF: a road to inflammation. *Nat Rev Immunol*. 2023;23(5):289–303. doi:10.1038/s41577-022-00792-3
36. Liu T, Zhang L, Joo D, Sun SC. NF- $\kappa$ B signaling in inflammation. *Signal Transduct Target Ther*. 2017;2:17023. doi:10.1038/sigtrans.2017.23
37. Zhuang M, Scholz A, Walz G, Yakulov TA. Histone deacetylases cooperate with NF- $\kappa$ B to support the immediate migratory response after zebrafish pronephros injury. *Int J Mol Sci*. 2022;23(17):9582. doi:10.3390/ijms23179582
38. Edirisinghe SL, Rajapaksha DC, Nikapitiya C, et al. *Spirulina maxima* derived marine pectin promotes the in vitro and in vivo regeneration and wound healing in zebrafish. *Fish Shellfish Immunol*. 2020;107(PA):414–425. doi:10.1016/j.fsi.2020.10.008
39. Xie Y, Meijer AH, Schaaf MJM. Modeling Inflammation in Zebrafish for the development of anti-inflammatory drugs. *Front Cell Dev Biol*. 2021;8. doi:10.3389/fcell.2020.620984
40. Herbomel P. Spinning nuclei in the brain of the zebrafish embryo [1]. *Curr Biol*. 1999;9(17):3735–3745. doi:10.1016/S0960-9822(99)80407-2
41. Hermann AC, Millard PJ, Blake SL, Kim CH. Development of a respiratory burst assay using zebrafish kidneys and embryos. *J Immunol Methods*. 2004;292(1–2):119–129. doi:10.1016/j.jim.2004.06.016
42. Lieschke GJ, Oates AC, Crowhurst MO, Ward AC, Layton JE Morphologic and functional characterization of granulocytes and macrophages in embryonic and adult Zebrafish; 2001. Available from: <http://ashpublications.org/blood/article-pdf/98/10/3087/1678504/h8220103087.pdf>. Accessed July 24, 2024.
43. Naomi R, Bahari H, Yazid MD, Embong H, Othman F. Zebrafish as a model system to study the mechanism of cutaneous wound healing and drug discovery: advantages and challenges. *Pharmaceuticals*. 2021;14(10):1058. doi:10.3390/ph14101058
44. Bastakoty D, Young PP. Wnt/ $\beta$ -catenin pathway in tissue injury: roles in pathology and therapeutic opportunities for regeneration. *FASEB J*. 2016;30(10):3271–3284. doi:10.1096/fj.201600502R
45. Pizzi A. Tannins: prospectives and actual industrial applications. *Biomolecules*. 2019;9(8):344. doi:10.3390/biom9080344
46. Sarkar A, Bhaduri A. Black tea is a powerful chemopreventor of reactive oxygen and nitrogen species: comparison with its individual catechin constituents and green tea. *Biochem Biophys Res Commun*. 2001;284(1):173–178. doi:10.1006/bbrc.2001.4944
47. Hussain T, Tan B, Yin Y, Blachier F, Tossou MCB, Rahu N. Oxidative stress and inflammation: what polyphenols can do for us? *Oxid Med Cell Longev*. 2016;2016. doi:10.1155/2016/7432797
48. Hong J, Smith TJ, Ho CT, August DA, Yang CS. Effects of purified green and black tea polyphenols on cyclooxygenase- and lipoxygenase-dependent metabolism of arachidonic acid in human colon mucosa and colon tumor tissues. *Biochem Pharmacol*. 2001;62(9):1175–1183. doi:10.1016/S0006-2952(01)00767-5
49. Soyocak A, Kurt H, Cosan DT, et al. Tannic acid exhibits anti-inflammatory effects on formalin-induced paw edema model of inflammation in rats. *Hum Exp Toxicol*. 2019;38(11):1296–1301. doi:10.1177/0960327119864154
50. Morena AG, Bassegoda A, Natan M, Jacobi G, Banin E, Tzanov T. Antibacterial properties and mechanisms of action of sonoenzymatically synthesized lignin-based nanoparticles. *ACS Appl Mater Interfaces*. 2022;14(33):37270–37279. doi:10.1021/acsmi.2c05443
51. Watzke J, Schirmer K, Scholz S. Bacterial lipopolysaccharides induce genes involved in the innate immune response in embryos of the zebrafish (*Danio rerio*). *Fish Shellfish Immunol*. 2007;23(4):901–905. doi:10.1016/j.fsi.2007.03.004

52. Novoa B, Bowman TV, Zon L, Figueras A. LPS response and tolerance in the zebrafish (*Danio rerio*). *Fish Shellfish Immunol.* 2009;26(2):326–331. doi:10.1016/j.fsi.2008.12.004
53. Heusch M, Lin L, Geleziunas R, Greene WC. The generation of nfkb2 p52: mechanism and efficiency. *Oncogene.* 1999;18(46):6201–6208. doi:10.1038/sj.onc.1203022
54. Ziembowicz S, Kida M, Koszelnik P. Sonochemical formation of hydrogen peroxide. MDPI AG. 2017;188. doi:10.3390/ecws-2-04957.
55. Heo S, Kim S, Kang D. The role of hydrogen peroxide and peroxiredoxins throughout the cell cycle. *Antioxidants.* 2020;9(4):280. doi:10.3390/antiox9040280
56. Ransy C, Vaz C, Lombès A, Bouillaud F. Use of H<sub>2</sub>O<sub>2</sub> to cause oxidative stress, the catalase issue. *Int J Mol Sci.* 2020;21(23):1–14. doi:10.3390/ijms21239149
57. Danilova N, Wilkes M, Bibikova E, Youn MY, Sakamoto KM, Lin S. Innate immune system activation in zebrafish and cellular models of Diamond Blackfan Anemia. *Sci Rep.* 2018;8(1):1–11. doi:10.1038/s41598-018-23561-6
58. Kumar R, Butreddy A, Kommineni N, et al. Lignin: drug/gene delivery and tissue engineering applications. *Int J Nanomed.* 2021;16:2419–2441. doi:10.2147/IJN.S303462
59. Ullah I, Chen Z, Xie Y, et al. Recent advances in biological activities of lignin and emerging biomedical applications: a short review. *Int J Biol Macromol.* 2022;208:819–832. doi:10.1016/j.ijbiomac.2022.03.182
60. Baldwin A, Booth BW. Biomedical applications of tannic acid. *J Biomater Appl.* 2022;36(8):1503–1523. doi:10.1177/08853282211058099
61. Jafari H, Ghaffari-Bohlouli P, Niknezhad SV, et al. Tannic acid: a versatile polyphenol for design of biomedical hydrogels. *J Mater Chem B.* 2022;10(31):5873–5912. doi:10.1039/d2tb01056a
62. Zuñiga-Traslaviña C, Bravo K, Reyes AE, Fejjoó CG. Cxcl8b and Cxcr2 regulate neutrophil migration through bloodstream in Zebrafish. *J Immunol Res.* 2017;2017. doi:10.1155/2017/6530531
63. Edirisinghe SL, Rajapaksha DC, Nikapitiya C, et al. Spirulina maxima derived pectin nanoparticles enhance the immunomodulation, stress tolerance, and wound healing in Zebrafish. *Mar Drugs.* 2020;18(11):556. doi:10.3390/MD18110556
64. Fang J, Muto T, Kleppe M, et al. TRAF6 mediates basal activation of NF- $\kappa$ B necessary for hematopoietic stem cell homeostasis. *Cell Rep.* 2018;22(5):1250–1262. doi:10.1016/j.celrep.2018.01.013
65. Tanaka T, Narazaki M, Kishimoto T. Il-6 in inflammation, Immunity, and disease. *Cold Spring Harb Perspect Biol.* 2014;6(10):a016295. doi:10.1101/cshperspect.a016295
66. Beissert S, Hosoi J, Kühn R, Rajewsky K, Müller W, Granstein RD. Impaired immunosuppressive response to ultraviolet radiation in interleukin-10-deficient mice. *J Invest Dermatol.* 1996;107(4):553–557. doi:10.1111/1523-1747.ep12582809
67. Brink N, Szamel M, Young AR, Wittern KP, Bergemann J. Comparative quantification of IL-1 $\beta$ , IL-10, IL-10r, TNF $\alpha$  and IL-7 mRNA levels in UV-irradiated human skin in vivo. *Inflammation Res.* 2000;49(6):290–296. doi:10.1007/PL00000209
68. Banerjee S, Leptin M. Systemic response to ultraviolet radiation involves induction of leukocytic IL-1 $\beta$  and inflammation in Zebrafish. *J Immunol.* 2014;193(3):1408–1415. doi:10.4049/jimmunol.1400232
69. Paredes-Zuñiga S, Morales RA, Muñoz-Sánchez S, et al. CXCL12a/CXCR4b acts to retain neutrophils in caudal hematopoietic tissue and to antagonize recruitment to an injury site in the zebrafish larva. *Immunogenetics.* 2017;69(5):341–349. doi:10.1007/s00251-017-0975-9
70. Myllymäki H, Yu P, Feng Y. Opportunities presented by zebrafish larval models to study neutrophil function in tissues. *Int J Biochem Biotechnol.* 2022;148:106234. doi:10.1016/j.biocel.2022.106234
71. Petrie TA, Strand NS, Yang CT, Rabinowitz JS, Moon RT. Macrophages modulate adult zebrafish tail fin regeneration. *Development.* 2015;142(2):406. doi:10.1242/dev.120642
72. Xu Y, Liu J, Tian Y, et al. Wnt/ $\beta$ -catenin signaling pathway is strongly implicated in cadmium-induced developmental neurotoxicity and neuroinflammation: clues from Zebrafish neurobehavior and in vivo neuroimaging. *Int J Mol Sci.* 2022;23(19):11434. doi:10.3390/ijms231911434
73. Bastakoty D, Saraswati S, Cates J, Lee E, Nanney LB, Young PP. Inhibition of Wnt/ $\beta$ -catenin pathway promotes regenerative repair of cutaneous and cartilage injury. *FASEB J.* 2015;29(12):4881–4892. doi:10.1096/fj.15-275941
74. Boudjou S, Oomah BD, Zaidi F, Hosseinian F. Phenolics content and antioxidant and anti-inflammatory activities of legume fractions. *Food Chem.* 2013;138(2–3):1543–1550. doi:10.1016/j.foodchem.2012.11.108
75. Bhaskar S, Helen A. Quercetin modulates toll-like receptor-mediated protein kinase signaling pathways in oxLDL-challenged human PBMCs and regulates TLR-activated atherosclerotic inflammation in hypercholesterolemic rats. *Mol Cell Biochem.* 2016;423(1–2):53–65. doi:10.1007/s11010-016-2824-9
76. Qiang M, Kinner K. Chemoprotection by phenolic antioxidants. Inhibition of tumor necrosis factor  $\alpha$  induction in macrophages. *J Biol Chem.* 2002;277(4):2477–2484. doi:10.1074/jbc.M106685200
77. Pizzi A. Tannins medical / pharmacological and related applications: a critical review. *Sustain Chem Pharm.* 2021;22. doi:10.1016/j.secp.2021.100481